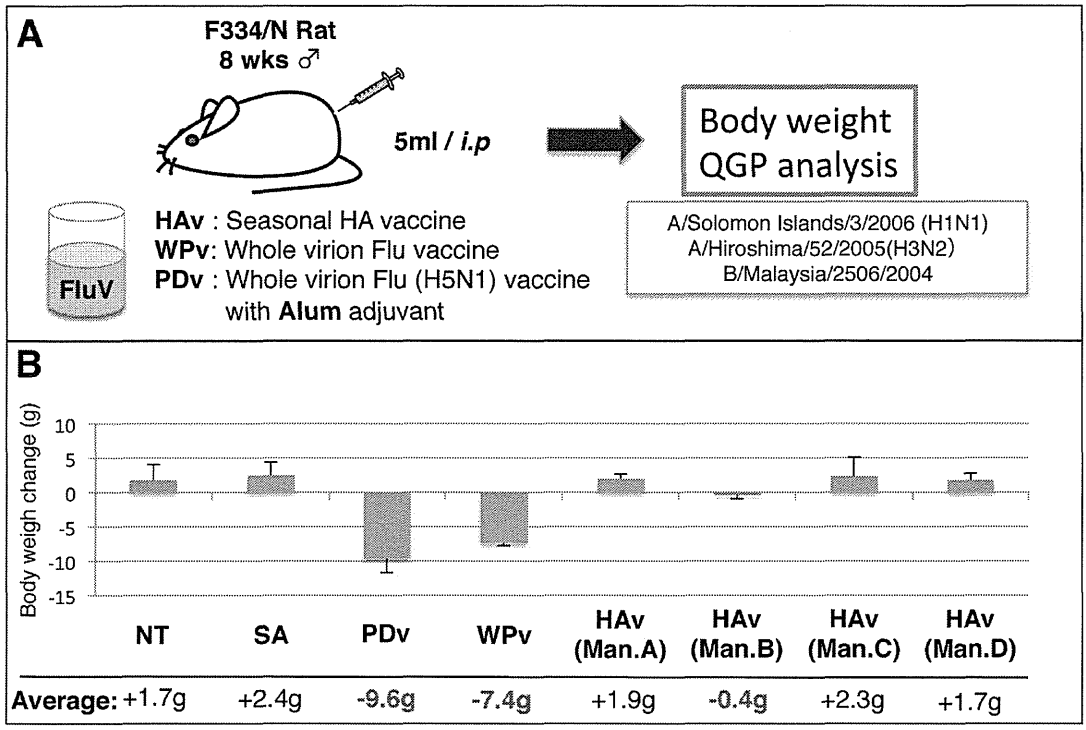

Figure 3. Evaluation of seasonal influenza vaccine with conventional animal safety test. A) The abnormal toxicity test was performed according to the Minimum Requirements of Biological Products. Each 5 ml vaccine was *i.p.* injected into rats, the body weight measured and lung tissues collected at day 1 after injection. B) Body weight change at day 1 after injection. NT: nontreated rat, SA: saline, PDv: pandemic H5N1 whole virion-derived vaccine with alum adjuvant, WPv: whole particle virion influenza vaccine, HAv: influenza HA vaccine, Man: manufacturer.
doi:10.1371/journal.pone.0101835.g003

used in a 20-μl final volume reaction containing 10 μl SYBR Green PCR Master Mix (Applied Biosystems), and forward and reverse primers were as described previously [13]. The 7500 Fast System was programmed to run an initial polymerase activation step at 95°C for 10 min followed by 40 cycles of denaturation (95°C for 15 s) and extension (60°C for 1 min). Product synthesis was monitored at the end of the extension step of each cycle. Gene expression values were normalized against rat GAPDH.

6. QuantiGene Plex assays

QuantiGene Plex (QGP) assays were performed according to the QuantiGene Plex Reagent System instructions (Panomics Inc., Fremont, CA), as described previously [11]. Briefly, 10 μl of starting poly (A)+RNA (50 ng) was incubated for 10 min at 65°C, then mixed with 33.3 μl of lysis mixture, 40 μl of capture buffer, 2 μl of capture beads, and 2 μl of the target gene-specific probe set. Probe sets were heated for 5 min prior to use. Each sample mixture was then dispensed into an individual well of a capture plate, sealed with foil tape and incubated at 54°C for 16–20 h. The hybridization mixture was transferred to a filter plate, and the wells were washed three times with 200 μl of wash buffer. Signals for the bound target mRNA were developed by sequential hybridization with branched DNA (bDNA) amplifier, and biotin-conjugated label probe, at 48°C for 1 h each. Two washes with wash buffer were used to remove unbound material after each hybridization step. Streptavidin-conjugated phycoerythrin was added to the wells and incubated at room temperature for 30 min. The luminescence of each well was measured using a Luminex 100 microtiter plate luminometer (Luminex). Two replicate assays measuring RNA directly (independent sampling n = 6 for mRNA, n = 3–5 for lysate) were performed for all described experiments. The 20 target genes and GAPDH mRNA were quantified, and the ratio of the target genes to GAPDH mRNA was calculated.

7. Statistical analysis

Multiple comparisons were performed for SA, PDv, WPv and HA. To determine differences between manufacturers, multiple comparisons were performed for SA and HA from manufacturers A, B, C and D. Statistical analysis was performed in GraphPad Prism 6 (GraphPad Software, La Jolla, CA) using an ordinary one-way analysis of variance test followed by a Tukey multiple comparison test.

Results

Optimization of multiple gene detection system, QuantiGene Plex, for safety evaluation of the influenza vaccine

We previously reported that 20 selected genes (**Table 1**), from 76 differentially expressed genes in adsorbed PDv-treated rats, could be used as biomarkers to evaluate H5N1 influenza vaccine safety compared with other types of influenza vaccine using conventional real-time PCR [13]. To establish faster and more convenient methods to detect these biomarkers in one-step as a new vaccine safety test, we used QuantiGene Plex (QGP)

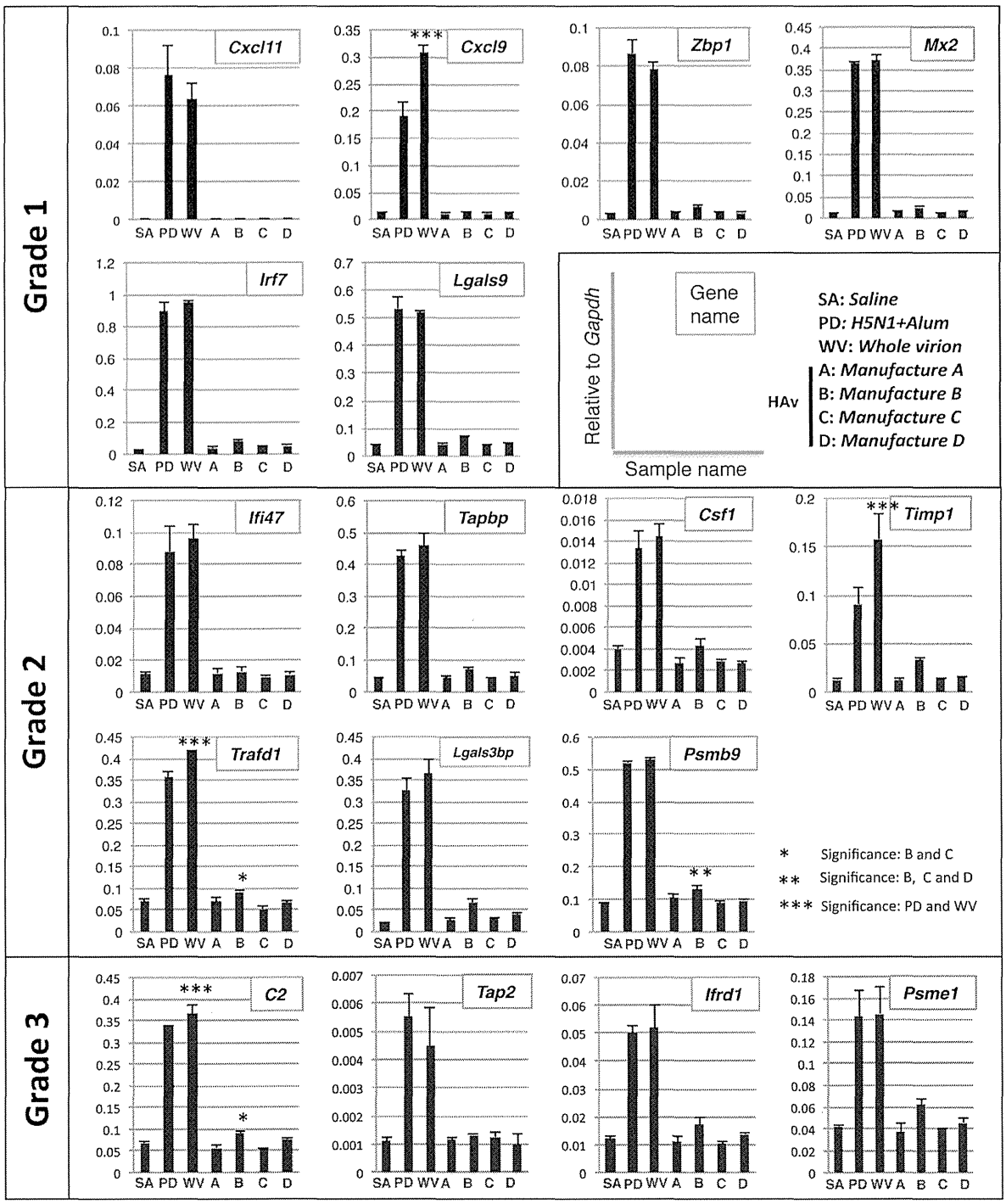

Figure 4. Evaluation of seasonal influenza vaccine with QGP. The relative gene expression levels of the *Gapdh* gene are indicated in each column (grades 1, 2 and 3, respectively). *Significant difference between B and C. **Significant difference between B, C and D, ***Significant difference between PD and WPv.
doi:10.1371/journal.pone.0101835.g004

technology (Panomics Inc., Fremont, CA). We designed a custom QGP 2.0 assay to enable the measurement of expression levels of identified biomarkers. The Panomics QGP 2.0 assays provided quantitative measurements of 3 to 80 target RNAs per well by

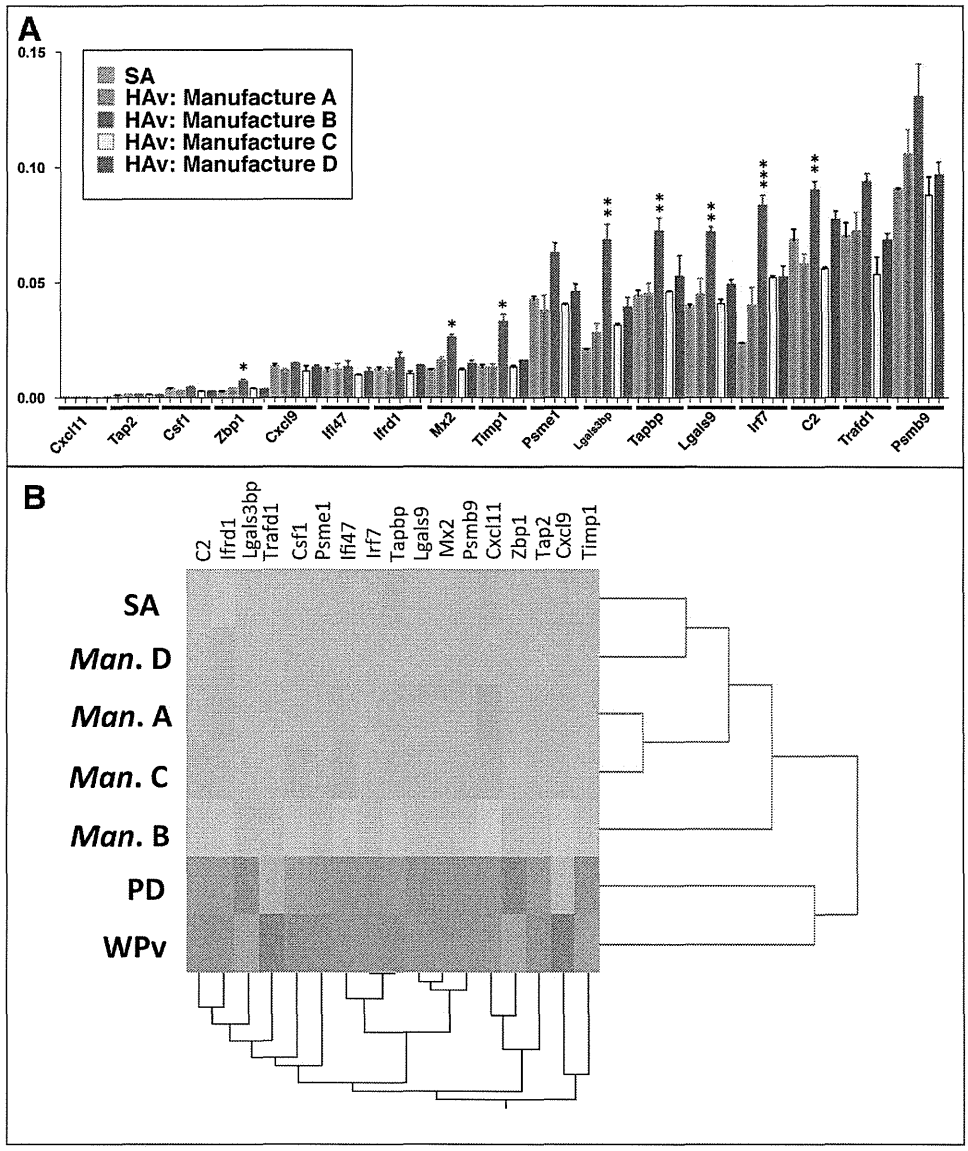

Figure 5. Evaluation of seasonal influenza vaccine with QGP and cluster analysis. A) Relative gene expression in HAv-treated rat lungs to *Gapdh* is indicated in the bar graph. B) Hierarchical clustering analysis with biomarkers could predict differences in HAv manufacturers as B is located in a separate cluster from other HAvs.
doi:10.1371/journal.pone.0101835.g005

using bDNA technology in conjunction with multi-analyte magnetic beads to provide the detection and quantitation of multiple mRNA targets simultaneously. bDNA technology is a hybridization-based methodology that uses labeled DNA probes to amplify the signal rather than the target mRNA. Here, we produced probes for 20 genes and two control genes (*Actb* and *Gapdh*) for the one-step detection and quantification of these biomarkers. To check the sensitivity of probes and dynamic range of our biomarkers, we prepared 0.02, 0.2, 2 and 20 ng total RNA samples from WPv and SA-treated rat lungs and performed QGP analysis. Two control genes and two biomarkers (*β2m* and *C2*) reacted in a dose-dependent manner (**Figure 1A**). We re-evaluated all probes with the same sample. Each biomarker reacted in a dose-dependent manner (**Figure 1B**) except *Ngfr* and *Npc1*. Therefore, 20 ng of RNA sample was used for multiplex gene detection. All biomarkers except *β2m* reacted in a dose-dependent manner. *β2m* was saturated when using 20 ng RNA sample; thus *β2m* could not be used for QGP analysis.

Validation of QGP with real-time PCR

To validate QGP, we performed real-time PCR analysis using the same samples. As a result, most biomarker gene expression data from the QGP correlated with the real-time PCR result except for *β2m*, *Npc1* (Figure 2) and *Ngfr* (data not shown). Finally,

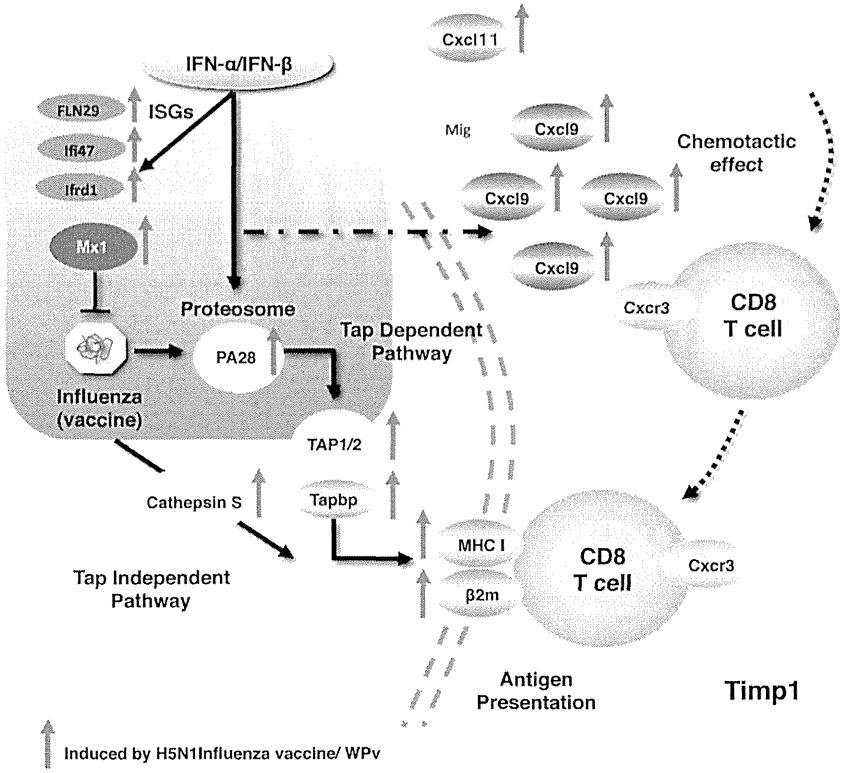

Figure 6. Summary of biomarker studies. Biomarkers used in this study were strongly correlated with immune responses after influenza infection.
doi:10.1371/journal.pone.0101835.g006

17 genes were selected as the multiplex detection biomarker set. We next determined the relative biomarker expression levels in HAv-treated rat lungs compared with WPv used as a reference toxicity vaccine in the leukopenic toxicity test (LTT) in Japan. We classified *Cxcl11*, *Cxcl9*, *Zbp1*, *Mx2*, *Ifi7* and *Lgals9* as a "Grade 1" gene set where relative expression levels in HAv compared with WPv were less than 10%. Likewise, we classified *Ifi47*, *Tapbp*, *Csf1*, *Timp1*, *Trafd1*, *Lgals3bp* and *Psmb9* as a "Grade 2" gene set where relative expression levels were less than 20% and *C2*, *Tap2*, *Ifrd1* and *Psme1* as a "Grade 3" gene set where relative expression levels were less than 40% in HAv compared with WPv. In Japan, it is acceptable for leukopenic toxicity levels of HAv to be not more than 20% of WPv by LTT. We applied LTT criteria for selecting and subdividing these biomarkers into three grades with expression levels below 20% of WPv and others.

Evaluation of HAv safety in Japan using ATT and QGP

To evaluate the toxicity of seasonal HAv using biomarkers, we purchased market authorized seasonal influenza vaccines distributed in Japan from four different manufacturers (Kaketsuken, Denka Seiken, Kitasato, and Biken). Although the vaccines have been evaluated and passed ATT by the NCL according to the Japanese guidelines for MRBP, the reactogenicity of the vaccine to animals (rats, mice and guinea pigs) was varied. To evaluate these differences, we performed ATT and checked the body weight changes of rats after *i.p.* injection of each HAv (Figure 3A). Although treatment with PDv or WPv (toxic reference whole virion-derived vaccines) significantly decreased the body weight of rats, HAvs from three different manufacturers had no effect on body weight. HAv from manufacture B reduced the body weight of rats at day 1 (Figure 3B). However, there was no significant difference in rat body weight change for the other HAvs; thus HAv from manufacturer B might be slightly different, when comparing the mean body weight at day 1. In addition, there was no significant difference in leukocyte numbers following administration of HAv from the four manufacturers (data not shown). To evaluate the differences of each HAv, we next performed multiplex biomarker detection by QGP. No biomarkers were significantly up-regulated in HAv-treated rats compared with controls (Figure 4) except for *Psmb9*. Furthermore, *Psmb9* expression was significantly up-regulated following administration of HAv from manufacturer B compared with the control SA-treated and HAvs from the other manufacturers. The expression levels of *C2* and *Trafd1* were also significantly up-regulated in the HAv from manufacturer B compared with the HAv from manufacturer C.

Biomarkers to evaluate safety of adjuvanted influenza vaccine

Both PDv and WPv contain the whole virion influenza vaccine and alum adjuvant is only added to PDv to enhance its immunogenicity. There was no difference in body weight change between WPv- and PDv-treated rats (Figure 3B). However, among the 17 biomarkers, the expression level of three genes, *Cxcl9*, *Timp1* and *Trafd1* in PDv-treated rats were significantly decreased compared with WPv-treated rats (Figure 4). Thus, these biomarkers could potentially evaluate the aluminum adjuvant effect.

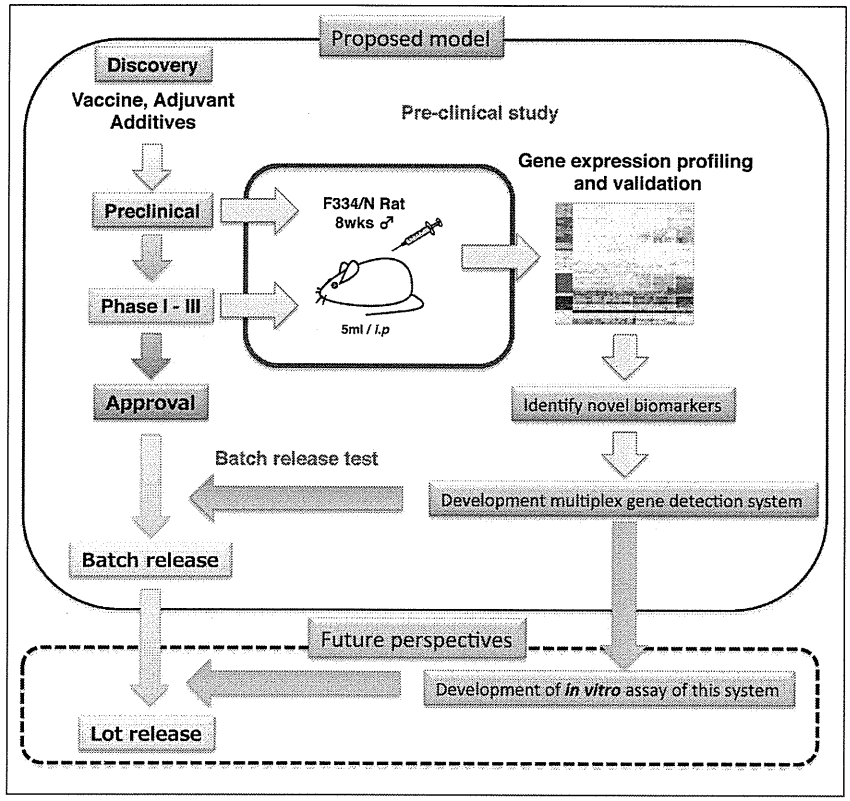

Figure 7. Application of the system biological approach for influenza vaccine development. Proposed model of future influenza vaccine development and establishment of preclinical studies and batch release testing. Acquisition of transcriptome data at the preclinical and clinical phase is useful for future batch release testing and the prediction of vaccine efficacy and toxicity.
doi:10.1371/journal.pone.0101835.g007

Cluster analysis of QGP data predicts influenza vaccine safety

Conventional animal tests such as ATT and LTT have been performed in Japan for the evaluation of influenza vaccine safety and toxicity. Despite applying these tests that evaluate whole virion-derived influenza vaccine from HAv, it is difficult to distinguish statistically between different HAvs if they do not have comparable toxicity greater than 20–50% to WPv. According to the body weight change observed with ATT, we speculated that HAv from manufacturer B was slightly different than the others tested (Figure 3B), although this was not statistically significant. However, when biomarkers were used with QGP to evaluate HAvs, we could distinguish the HAv from manufacturer B compared with those from other manufacturers. When we focused on biomarker expression among the HAv-treated rat lungs, the expression levels of *Zbp1*, *MX2*, *Timp1*, *Lgals3bp*, *Tapbp*, *Lgals9*, *Irf7* and *C2* were significantly up-regulated in rat lungs treated with HAvs from manufacturer B (Figure 5A). In addition, cluster analysis with the biomarkers predicted differences in HAvs as the vaccine from manufacturer B was located in a separate cluster from the other HAvs. Thus, these biomarkers can evaluate batch-to-batch and manufacturer-to-manufacturer differences in HAvs (Figure 5B).

Discussion

Vaccine safety is critical in the process of vaccine development and universal vaccination. Several vaccines were stopped owing to safety concerns, including severe side effects, after they had received marketing authorization and licensing, even when they were effective [14]. To ensure the safety of vaccines, the preclinical phase in the development of vaccines and the batch release system after marketing authorization is critical. However, the guidelines for nonclinical assessment of vaccines and batch release tests only focus on the evaluation of vaccine efficacy and immunogenicity in animal models, quality control testing programs and toxicology testing in relevant animal models [15]. These guidelines do not include scientific research for identifying the potential toxicities of the vaccines, adjuvants and additives.

We have demonstrated the advantage of a system biological approach using several vaccines authorized in Japan, *e.g.* DPT, JEV and Influenza vaccine including H5N1 pandemic influenza vaccine [10–13]. We successfully identified several biomarkers to evaluate DPT, JEV and influenza vaccine toxicity. In this study, we demonstrate that the biomarkers used to evaluate H5N1 pandemic influenza vaccine could also be used to evaluate the batch-to-batch consistency and the safety of HAvs. In addition, they can be used to evaluate manufacturer-to-manufacturer differences using the multiplex gene detection system. The biomarker analysis correlated to findings from conventional

animal use tests, such as ATT. In addition, sensitivity of toxicity detection and differences in HAvs was higher and more accurate than with conventional methods. Despite all the HAvs evaluated in this study meeting MRBP criteria and passing NCL, our results suggest that HAv from manufacturer B is slightly different than the HAvs according to *Lgals3bp*, *Tapbp*, *Lgals9*, *Irf7* and *C2* gene expression. Among the official vaccine adverse event information provided by the Japanese authorities, there is no reported evidence that the adverse event rate was increased or that severe adverse events were observed caused by HAv from manufacturer B. It is still unknown what factors (additives, formalin content, protein content) induce these biomarkers in the HAv from manufacturer B. Further studies are needed to determine whether our biomarkers could predict the toxicity of influenza vaccine by using different formulations of HAv. Using biomarkers from any grade characterized in this study, we could also predict the safety of influenza vaccines within 2 days whereas the conventional animal use safety test, ATT requires 7 days for evaluating batch-to-batch consistency and vaccine safety. Further studies are needed to determine how these biomarkers can be used to evaluate the safety of HAv. To set the percent limit of up-regulation of each biomarker, it might be helpful to compare another conventional test such as LTT [[http://www.nih.go.jp/niid/en/mrbp-e.html]] as well as a comparison of failed batches of HAv. LTT evaluates the peripheral leukocyte number reduction rate compared with WPv. In general, WPv induces a strong loss of peripheral leukocyte numbers 16 hours after WPv administration in mice [9 and 28]. The test criteria of LTT is that the loss of leukocyte numbers in test samples must be no greater than 20% compared with a reference toxic vaccine such as WPv or less than 50% of SA-treated mice. These criteria may be applicable to set our biomarker expression limit. Further validation is required to set the limit the gene expression level.

Influenza is a socially important infectious disease that causes seasonal flu outbreaks worldwide and has a pandemic status [16]. Correspondingly, many types of influenza vaccine (cell derived, recombinant derived, live attenuated and inactivated influenza vaccine), have been developed to ensure efficacy and reduce toxicity [17]. While some adjuvants have been developed and used to amplify vaccine efficacy [8], the safety of adjuvants is still of concern. Recently, several adjuvants (squalene-based MF59 and AS03) developed and licensed for use only in pandemic influenza vaccines were under investigation for the occurrence of narcolepsy in vaccinated children in European countries [18]. Conventional safety tests could be used to evaluate the safety of these vaccines [19], but it is still difficult to predict the safety and toxicity of influenza vaccines, adjuvants and additives [20]. We demonstrated that usage of system biological approaches to evaluate safety might revolutionize vaccine testing methods [21]. Most of the previously identified biomarkers were up-regulated and correlated with influenza infection, interferon responses, antigen presentation and antibody production (Figure 6). In addition, we found that several biomarkers, *Cxcl9*, *Trafd1*, and *C2* were candidates for evaluating differences between alum-adjuvanted influenza vaccines and nonadjuvanted vaccines. Further studies, using several adjuvants, are needed to confirm the feasibility of these biomarkers in evaluating adjuvant safety.

In addition to whole transcriptome analysis of vaccinated animals, recent advances in genome research enabled the acquisition of whole transcriptional data from vaccinated individuals and identification of gene expression after immunization with vaccines to yellow fever, measles, tularemia and tuberculosis [22]. With a focus on the influenza vaccine, Bucasas et al. reported a 494 gene set, including biomarkers identified in our previous study (*MX1*, *IRF7*) that strongly correlated with antibody responses in humans [23]. Wei et al. reported gene expression differences between HAv and live attenuated influenza vaccine. They identified 265 differentially expressed genes, including our previously identified biomarkers, *IRF7*, *MX1*, *MX2*, *OAS1* and *ZBP1* [24].

Recently, Nakaya and Pulendran reported a system biological approach, termed systems vaccinology [25], which was used to predict immunogenicity and provide new mechanistic insights regarding influenza vaccination. They also reported several gene sets that predicted influenza vaccine immunogenicity, including our previously identified biomarkers, *MX1*, *MX2*, *OAS1* and *IRF7* [26]. More recently, Franco et al. reported 20 genes, including our biomarkers, *TAP2* and *OAS1*, which correlated with antibody responses, using integrative genomic analysis [27]. All these reports suggest that using animal models is still useful if biomarkers are up-regulated in vaccinated individuals and can reveal the role of biomarkers in immune responses and vaccination toxicity. Thus, in the preclinical and clinical phase, the acquisition of transcriptome data from both vaccinated individuals and animals, and a comparison of these data will be helpful for future vaccine development and batch release testing (Figure 7).

Taken together, system biological approaches to identify vaccine toxicity using whole genome transcriptome methods will improve vaccine development in preclinical and clinical phases if more data are generated from successfully vaccinated individuals and those with side effects. It is still unclear whether and how these factors determine immunogenicity and toxicity. Further studies are required to identify and reveal the mechanisms underlying vaccination in humans and in animal models, including nonhuman primates.

Acknowledgments

The authors acknowledge Dr. Shinya Watanabe, Junichi-Imai for technical support of the initial transcriptome analysis after influenza vaccination of rats. The authors wish to thank Dr. Hiroshi Yamada for his advice on performing toxicogenomic studies.

Author Contributions

Conceived and designed the experiments: TM. Performed the experiments: TM HM MK KT. Analyzed the data: TM HM KJI IH KY. Contributed reagents/materials/analysis tools: TM HM MK KT KA KF KJI. Wrote the paper: TM.

References

1. Plotkin SL, Plotkin SA (2012) A short history of vaccination. General aspects of vaccination. In: Plotkin SA, Orenstein WA, Offit PA, editors. 6th edition Vaccines. Philadelphia: Saunders Elsevier. 1–13.
2. Baylor NW, Marshall VB (2012) Regulation and testing of vaccines. In: Plotkin SA, Orenstein WA, Offit PA, editors. 6th edition Vaccines. Philadelphia: Saunders Elsevier. 1427–1446.
3. Kurokawa M, Murata R (1961) On the Toxicity of the Toxoid Preparation Responsible for the Kyoto Catastrophe in 1948. Jpn J Med Sci Biol 14: 249–256.
4. Wood JM, Williams MS (1998) History of inactivated influenza vaccines. In: Nicholson KG, Webster RG, Hay AJ, editors. Textbook of influenza. Oxford: Blackwell Science. 317–323.
5. Nicholson KG, Tyrrell DA, Harrison P, Potter CW, Jennings R, et al. (1979) Clinical studies of monovalent inactivated whole virus and subunit A/USSR/77 (H1N1) vaccine: Serological responses and clinical reactions. J Biol Stand 7: 123–136.
6. Wright PF, Thompson J, Vaughn WK, Folland DS, Sell SH, et al. (1977) Trials of influenza A/New Jersey/76 virus vaccine in normal children: an overview of age-related antigenicity and reactogenicity. J Infect Dis 136: S731–S741.

7. Couch RB, Keitel WA, Cate TR (1997) Improvement of inactivated influenza virus vaccines. J Infect Dis. 176 Suppl 1: S38–44.
8. Even-Or O, Samira S, Ellis R, Kedar E, Barenholz Y (2013) Adjuvanted influenza vaccines. Expert Rev Vaccines. 12: 1095–1108.
9. Mizukami T, Masumi A, Momose H, Kuramitsu M, Takizawa K, et al. (2009) An improved abnormal toxicity test by using reference vaccine-specific body weight curves and histopathological data for monitoring vaccine quality and safety in Japan. Biologicals. 37: 8–17.
10. Hamaguchi I, Imai J, Momose H, Kawamura M, Mizukami T, et al. (2007) Two vaccine toxicity-related genes Agp and Hpx could prove useful for pertussis vaccine safety control. Vaccine. 25: 3355–3364.
11. Hamaguchi I, Imai J, Momose H, Kawamura M, Mizukami T, et al. (2008) Application of quantitative gene expression analysis for pertussis vaccine safety control. Vaccine. 26: 4686–4696.
12. Momose H, Imai J, Hamaguchi I, Kawamura M, Mizukami T, et al. (2010) Induction of indistinguishable gene expression patterns in rats by Vero cell-derived and mouse brain-derived Japanese encephalitis vaccines. Jpn J Infect Dis. 63: 25–30.
13. Mizukami T, Imai J, Hamaguchi I, Kawamura M, Momose H, et al. (2008) Application of DNA microarray technology to influenza A/Vietnam/1194/2004 (H5N1) vaccine safety evaluation. Vaccine. 26: 2270–2283.
14. Offit PA, Stefano FD (2012) Vaccine safety. In: Plotkin SA, Orenstein WA, Offit PA, editors. 6th edition Vaccines. Philadelphia: Saunders Elsevier. 1464–1480.
15. Wolf JJ, Kaplanski CV, Lebron JA (2010) Nonclinical safety assessment of vaccines and adjuvants. Methods Mol Biol. 626: 29–40.
16. WHO (2013) Pandemic Influenza Risk Management, WHO Interim Guidance. Available: http://www.who.int/influenza/preparedness/pandemic/GIP_PandemicInfluenzaRiskManagementInterimGuidance_Jun2013.pdf. Accessed 2014 June 18.
17. Wong SS, Webby RJ (2013) Traditional and new influenza vaccines. Clin Microbiol Rev. 26: 476–492.
18. Ahmed SS, Schur PH, Macdonald NE, Steinman L (2014). Narcolepsy, 2009 A (H1N1) pandemic influenza, and pandemic influenza vaccinations: What is known and unknown about the neurological disorder, the role for autoimmunity, and vaccine adjuvants. J Autoimmun. 50: 1–11.
19. Brennan FR1, Dougan G (2005) Non-clinical safety evaluation of novel vaccines and adjuvants: new products, new strategies. Vaccine. 23: 3210–3222.
20. Verdier F, Morgan L (2001) Predictive value of pre-clinical work for vaccine safety assessment. Vaccine. 20 Suppl 1: S21–23.
21. Momose H, Mizukami T, Ochiai M, Hamaguchi I, Yamaguchi K (2010) A new method for the evaluation of vaccine safety based on comprehensive gene expression analysis. J Biomed Biotechnol. 2010: 361841.
22. Wang IM, Bett AJ, Cristescu R, Loboda A, ter Meulen J (2012) Transcriptional profiling of vaccine-induced immune responses in humans and non-human primates. Microb Biotechnol. 5: 177–187.
23. Bucasas KL, Franco LM, Shaw CA, Bray MS, Wells JM, et al. (2011) Early patterns of gene expression correlate with the humoral immune response to influenza vaccination in humans. J Infect Dis. 203: 921–929.
24. Zhu W, Higgs BW, Morehouse C, Streicher K, Ambrose CS, et al. (2010) A whole genome transcriptional analysis of the early immune response induced by live attenuated and inactivated influenza vaccines in young children. Vaccine. 28: 2865–2876.
25. Pulendran B, Li S, Nakaya HI (2010) Systems vaccinology. Immunity. 33: 516–529.
26. Nakaya HI, Wrammert J, Lee EK, Racioppi L, Marie-Kunze S, et al. (2011) Systems biology of vaccination for seasonal influenza in humans. Nat Immunol. 12: 786–795.
27. Franco LM, Bucasas KL, Wells JM, Niño D, Wang X, et al. (2013) Integrative genomic analysis of the human immune response to influenza vaccination. Elife. 2: e00299.
28. Ato M, Takahashi Y, Fujii H, Hashimoto S, Kaji T, et al. (2013) Influenza A whole virion vaccine induces a rapid reduction of peripheral blood leukocytes via interferon-α-dependent apoptosis. Vaccine. 31: 2184–2190.

Hindawi Publishing Corporation
BioMed Research International
Volume 2014, Article ID 158128, 6 pages
http://dx.doi.org/10.1155/2014/158128

Hindawi

Research Article

The Early Activation of CD8$^+$ T Cells Is Dependent on Type I IFN Signaling following Intramuscular Vaccination of Adenovirus Vector

Masahisa Hemmi,[1] Masashi Tachibana,[1] Sayaka Tsuzuki,[1] Masaki Shoji,[1] Fuminori Sakurai,[1,2] Kenji Kawabata,[3] Kouji Kobiyama,[4,5] Ken J. Ishii,[4,5] Shizuo Akira,[6,7] and Hiroyuki Mizuguchi[1,8,9,10]

[1] *Laboratory of Biochemistry and Molecular Biology, Graduate School of Pharmaceutical Sciences, Osaka University, 1-6 Yamadaoka, Suita, Osaka 565-0871, Japan*
[2] *Laboratory of Regulatory Sciences for Oligonucleotide Therapeutics, Clinical Drug Development Unit, Graduate School of Pharmaceutical Sciences, Osaka University, 1-6 Yamadaoka, Suita, Osaka 565-0871, Japan*
[3] *Laboratory of Stem Cell Regulation, National Institute of Biomedical Innovation, 7-6-8 Asagi, Saito, Ibaraki, Osaka 567-0085, Japan*
[4] *Laboratory of Adjuvant Innovation, National Institute of Biomedical Innovation, 7-6-8 Asagi, Saito, Ibaraki, Osaka 567-0085, Japan*
[5] *Laboratory of Vaccine Science, World Premier International Research Center Immunology Frontier Research Center, Osaka University, 3-1 Yamadaoka, Suita, Osaka 565-0871, Japan*
[6] *Laboratory of Host Defense, World Premier International Research Center Immunology Frontier Research Center, Osaka University, 3-1 Yamadaoka, Suita, Osaka 565-0871, Japan*
[7] *Department of Host Defense, The Research Institute for Microbial Diseases, Osaka University, 3-1 Yamadaoka, Suita, Osaka 565-0871, Japan*
[8] *iPS Cell-Based Research Project on Hepatic Toxicity and Metabolism, Graduate School of Pharmaceutical Sciences, Osaka University, 1-6 Yamadaoka, Suita, Osaka 565-0871, Japan*
[9] *Laboratory of Hepatocyte Differentiation, National Institute of Biomedical Innovation, 7-6-8 Asagi, Saito, Ibaraki, Osaka 567-0085, Japan*
[10] *The Center for Advanced Medical Engineering and Informatics, Osaka University, 2-2 Yamadaoka, Suita, Osaka 565-0871, Japan*

Correspondence should be addressed to Hiroyuki Mizuguchi; mizuguch@phs.osaka-u.ac.jp

Received 19 March 2014; Accepted 14 May 2014; Published 27 May 2014

Academic Editor: Xin Ming

Few of the vaccines in current use can induce antigen- (Ag-) specific immunity in both mucosal and systemic compartments. Hence, the development of vaccines that realize both mucosal and systemic protection against various pathogens is a high priority in global health. Recently, it has been reported that intramuscular (i.m.) vaccination of an adenovirus vector (Adv) can induce Ag-specific cytotoxic T lymphocytes (CTLs) in both systemic and gut mucosal compartments. We previously revealed that type I IFN signaling is required for the induction of gut mucosal CTLs, not systemic CTLs. However, the molecular mechanism via type I IFN signaling is largely unknown. Here, we report that type I IFN signaling following i.m. Adv vaccination is required for the expression of type I IFN in the inguinal lymph nodes (iLNs), which are the draining lymph nodes of the administration site. We also showed that the type I IFN signaling is indispensable for the early activation of CTLs in iLNs. These data suggested that type I IFN signaling has an important role in the translation of systemic innate immune response into mucosal adaptive immunity by amplifying the innate immune signaling and activating CTLs in the iLN.

1. Introduction

Mucosal membranes have enormous surface areas, through which most pathogens access the body, and therefore, they are important in vaccine development to establish protective immune responses at mucosal sites as well as systemic sites [1, 2]. Hence, the development of vaccines that realize both

mucosal and systemic protection against various pathogens is a high priority in global health. However, few of the vaccines in current use can induce antigen- (Ag-) specific immunity in both mucosal and systemic compartments [3]. In general, the induction of mucosal immunity by systemic administration of vaccine has proven to be difficult due to the unique immunological features of the mucosal immune system [3].

The replication incompetent recombinant adenovirus vector (Adv) has several advantages as a gene therapy vector: it provides the highest gene transduction efficiency among the currently available vectors, it has low genotoxicity because it is not integrated into the chromosomal DNA, and it can be easily prepared in high titers. Moreover, it has been revealed that Adv can be applied to gene therapy-based vaccines, and several Adv and vaccine protocols have been used in preclinical studies [4]. Recently, it has been reported that intramuscular (i.m.) immunization with an Adv vaccine-expressing simian immunodeficiency virus (SIV) gag can induce functional and sustainable SIV gag-specific cytotoxic T lymphocytes (CTLs) in the gut mucosal compartments as well as the systemic compartments in mice and rhesus macaques [5–7]. Adv is expected to become a next generation mucosal vaccine that combats severe intracellular pathogens [8].

Innate immune responses have been clearly shown to be critical for the optimal induction of adaptive immune responses [9–11]. Moreover, there is accumulating evidence that the adjuvants which activate innate immunity are effective for the induction of vaccine effects [12]. Several studies have revealed that Adv-derived nucleic acids, adenoviral genomic DNA, and adenoviral noncoding RNA (virus-associated RNA (VA-RNA)) activate innate immunity and produce innate immune cytokines. The adenoviral genomic DNA triggers innate immune responses through several pattern recognition receptors and adaptor molecules, such as Toll-like receptor 9 (TLR9)/myeloid differentiation primary-response protein 88 (MyD88) [13–15], and cGAMP synthase (cGAS)/stimulator of interferon genes (STING) [16], and induces the production of type I IFNs and proinflammatory cytokines. VA-RNA also induces the production of type I IFN through IFN-β promoter stimulator-1 (IPS-1) [17]. Type I IFN induced by Adv immunization has been shown to have an important role in the subsequent systemic adaptive immunity. It is indicated that not only dendritic cells (DCs), but also other types of cells, such as stromal cells, produce IFN-β *in vivo* and are involved in the induction of adaptive immunity [17–19]. Thus, determining the role of IFN-β *in vivo* is important for vaccine development. Moreover, the magnitudes of type I IFN correlate with the titers of Ad-specific neutralizing antibodies, suggesting that type I IFN signaling controls the efficacy of Adv vaccine [20]. We previously reported that type I IFN signaling following i.m. Adv vaccination is required for the induction of Ag-specific CTLs not in the systemic compartment but in the gut mucosal compartment [8]. Thus, type I IFN is important for the positive regulation of the Ag-specific gut mucosal cellular immune response. However, it is unclear how the Adv-induced type I IFN signaling translates innate immune response into gut mucosal adaptive immunity.

In this study, we report that type I IFN signaling is indispensable for the expression of IFN-α, IFN-β, cGAS, and TLR9in the draining lymph nodes (DLNs) in the early stage following i.m. Adv vaccination. Moreover, we found that type I IFN signaling is essential for the early activation of $CD8^+$ T cells in the DLNs. These data suggested that type I IFN signaling has an important role in the translation of systemic innate immunity into mucosal adaptive immunity. Our findings should lead to the development of safer and more efficient mucosal Adv vaccines.

2. Materials and Methods

2.1. Mice. C57BL/6J (wild-type, WT) mice were purchased from Japan SLC (Hamamatsu, Japan) and $IFNAR2^{-/-}$ mice (C57BL/6J background) were established as described previously [21]. All mice were housed in an animal facility under specific pathogen-free conditions and used at 7-8 weeks of age. All animal experimental procedures used in this study were performed in accordance with the institutional guidelines for animal experiments at Osaka University and the National Institute of Biomedical Innovation.

2.2. Adv Production and Immunization. The adenovirus type 5 vector-expressing LacZ (Ad-LacZ) was constructed as described previously [22]. Briefly, the expression cassette containing the chicken β-actin promoter with the cytomegalovirus enhancer (CA) driven [23] LacZ gene was inserted into the E1/E3-deleted adenovirus type 5 genome. This virus was grown in 293 cells using standard techniques. Ad-LacZ was purified with $CsCl_2$ step gradient ultracentrifugation, dialyzed with a solution containing 10 mM Tris (pH 7.5), 1 mM $MgCl_2$, and 10% glycerol, and stored in aliquots at −80°C. Determination of the virus particle (vp) titers was accomplished spectrophotometrically according to the methods of Maizel et al. [24]. All mice were injected under anesthesia in the right and left quadriceps muscles with Ad-LacZ (5×10^9 vp per muscle; total 10^{10} vp per mouse).

2.3. Isolation of Mononuclear Cells. The inguinal lymph nodes and mesenteric lymph nodes were dissected and pressed through a 70 μm cell strainer. The cells were washed with FACS buffer (2% FCS, 0.02% sodium azide in PBS).

2.4. DNA Isolation and qPCR. Total DNA was isolated from whole tissues using a DNeasy Blood & Tissue Kit (QIAGEN). Quantitative PCR was performed with Taqman Fast Universal PCR Master Mix (Applied Biosystems) using an Applied Biosystem StepOnePlus Real-Time PCR System. Absolute quantities were calculated using standard curves. The copy numbers of each gene were normalized with those of GAPDH. The primer sequences in this study are Gapdh forward, 5′-CAATGTGTCCGTCGTGGATCT-3′; Gapdh reverse, 5′-GTCCTCAGTGTAGCCCAAGATG-3′; Ad E4 forward, 5′-GGGATCGTCTACCTCCTTTTGA-3′; Ad E4 reverse, 5′-GGGCAGCAGCGGATGAT-3′.

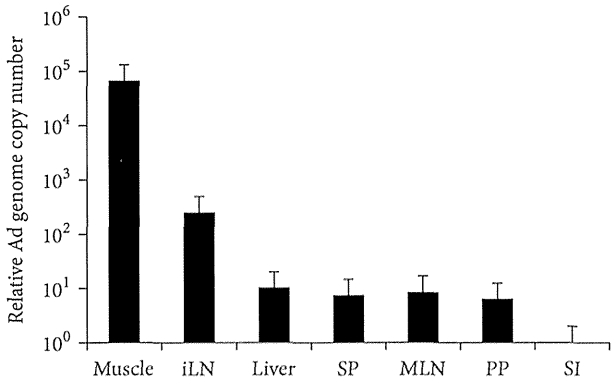

FIGURE 1: The tissue distribution of Adv following i.m. Adv vaccination. At 8 hours after the i.m. vaccination of 10^{10} vp of Ad-LacZ, the tissue distribution of Adv was determined by the absolute quantity of Ad E4 gene in each tissue, normalized by the copy number of GAPDH. The graphs represent the relative Ad genome copy number in each tissue normalized by that of the small intestine. Data are shown as the means ± S.E.M. (n = 3). iLN, inguinal lymph node; SP, spleen; MLN, mesenteric lymph node; PP, Peyer's patch; SI, small intestine.

2.5. RNA Isolation and RT-PCR. Total RNA was isolated from mononuclear cells using ISOGEN (Nippon Gene). cDNA was synthesized using 400 ng of total RNA with a Superscript VILO cDNA Synthesis Kit (Invitrogen) according to the manufacturer's instructions. Quantitative RT-PCR was performed with THUNDERBIRD qPCR Mix (TOYOBO) using an Applied Biosystem StepOnePlus Real-Time PCR System. Relative expression was calculated using the $\Delta\Delta C_T$ method. The mRNA level of each gene was normalized with that of β-actin. The primer sequences used in this study are *Actb* forward, 5′-GGCTGTATTCCCCTCCATCG-3′; *Actb* reverse, 5′-CCAGTTGGTAACAATGCCATGT-3′; *Ifna* forward, 5′-CTTCCACAGGATCACTGTGTACCT-3′; *Ifna* reverse, 5′-TTCTGCTCTGACCACCTCCC-3′; *Ifnb* forward, 5′-CTGGAGCAGCTGAATGGAAAG-3′; *Ifnb* reverse, 5′-CTTCTCCGTCATCTCCATAGGG-3′; *Mb21d1* forward, 5′-AGGAAGCCCTGCTGTAACACTTCT-3′; *Mb21d1* reverse, 5′-AGCCAGCCTTGAATAGGTAGTCCT-3′; *Tlr9* forward, 5′-ATGGTTCTCCGTCGAAGGACT-3′; *Tlr9* reverse, 5′-GAGGCTTCAGCTCACAGGG-3′; *Ddx41* forward, 5′-AGTCCGCCAAGGAAAAGCAA-3′; *Ddx41* reverse, 5′-CTCAGACATGCTCAGGACATAAC-3′; *Il1b* forward, 5′-GCAGCAGCACATCAACAAG-3′; *Il1b* reverse, 5′-CGGGAAAGACACAGGTAGC-3′; *Tnfa* forward, 5′-CCCTCACACTCAGATCATCTTCT-3′; *Tnfa* reverse, 5′-GCTACGACGTGGGCTACAG-3′.

2.6. Flow Cytometry. The antimouse antibodies used in this study were purchased from eBioscience (PE-Cy7-CD3ε (145-2C11)) and BioLegend (FITC-CD4 (GK1.5), APC-Cy7-CD8α (53-6.7), Pacific Blue-CD69 (H1.2F3)). Flow cytometry analysis was performed using a fluorescence-activated cell sorting (FACS) LSR Fortessa flow cytometer and BD FACSDiva software (BD Bioscience). Dead cells were excluded by 7-amino-actinomycin D staining (eBioscience).

2.7. Statistics. All results are shown as the mean ± standard error of the mean. Statistical significance was analyzed by the One-way ANOVA among groups.

3. Results

3.1. Adv Was Mainly Distributed to the Inguinal Lymph Nodes following i.m. Adv Vaccination. Innate immune responses are elicited within several hours after i.m. Adv vaccination. To reveal the sites where Adv induces the responses, we first examined Ad genome copy numbers in each tissue at 8 hours after i.m. Adv vaccination. Adv was mainly distributed to the muscles and inguinal lymph nodes (iLNs), the DLNs of the vaccination site (Figure 1). On the other hand, Adv was barely distributed to mesenteric lymph node (MLN), which is important for gut mucosal immunity. The distributions of Adv in the liver, spleen (SP), Peyer's patches (PP), and small intestine (SI) were similar to those in the MLN. These results suggested that Adv should induce innate immune responses in the iLNs.

3.2. Type I IFN Signaling Enhances the Expression of Innate Immune Cytokines and DNA Sensors in the Draining Lymph Nodes. Next, to reveal the roles of type I IFN signaling in the induction of gut mucosal CTLs, we examined the expression of innate immune cytokines and interferon-stimulated genes (ISGs) in iLNs and MLN by using type I IFN receptor knockout (IFNAR2 KO) mice, which have defects in immune responses to viruses and double-stranded DNA. In Adv-administrated WT mice, the expression of IFN-α and IFN-β was upregulated in the iLNs, where Adv was mainly distributed at this time point (Figure 2(a)). Moreover, in Adv-administrated WT mice, the expression of IL-1β and TNF-α tended to be upregulated in the iLNs (Figure 2(a)). On the other hand, the expression of these cytokines was not upregulated in the MLN, where Adv was barely distributed. Similarly, the expression of cGAS, a representative ISG, that is, encoded by *Mb21d1* [25], was upregulated in the iLNs (Figure 2(b)). However, in Adv-administrated IFNAR2 KO mice, the expression of IFN-α, IFN-β, and cGAS in the iLNs was not upregulated following i.m. Adv vaccination. In addition, in Adv-administrated IFNAR2 KO mice, the expression of IL-1β and TNF-α in the iLNs was lower than that in the iLNs of Adv-administrated WT mice.

Since cGAS is one of the DNA sensors detecting Ad genome [16], we next examined the expression of other DNA sensors, TLR9 and DDX41, which are widely known for sensing Ad genome [15, 26]. In Adv-administrated WT mice, only the expression of TLR9 was upregulated in the iLNs (Figure 2(c)). However, it was not upregulated in the iLNs of Adv-administrated IFNAR2 KO mice. These data suggested that type I IFN signaling enhances the expression of IFN-α, IFN-β, cGAS, and TLR9 in the iLNs, where much Adv is distributed from the muscles. It is speculated that the lack of type I IFN signaling in the innate immune responses at the iLNs leads to the significant reduction of antigen-specific CTLs in the gut mucosal compartment.

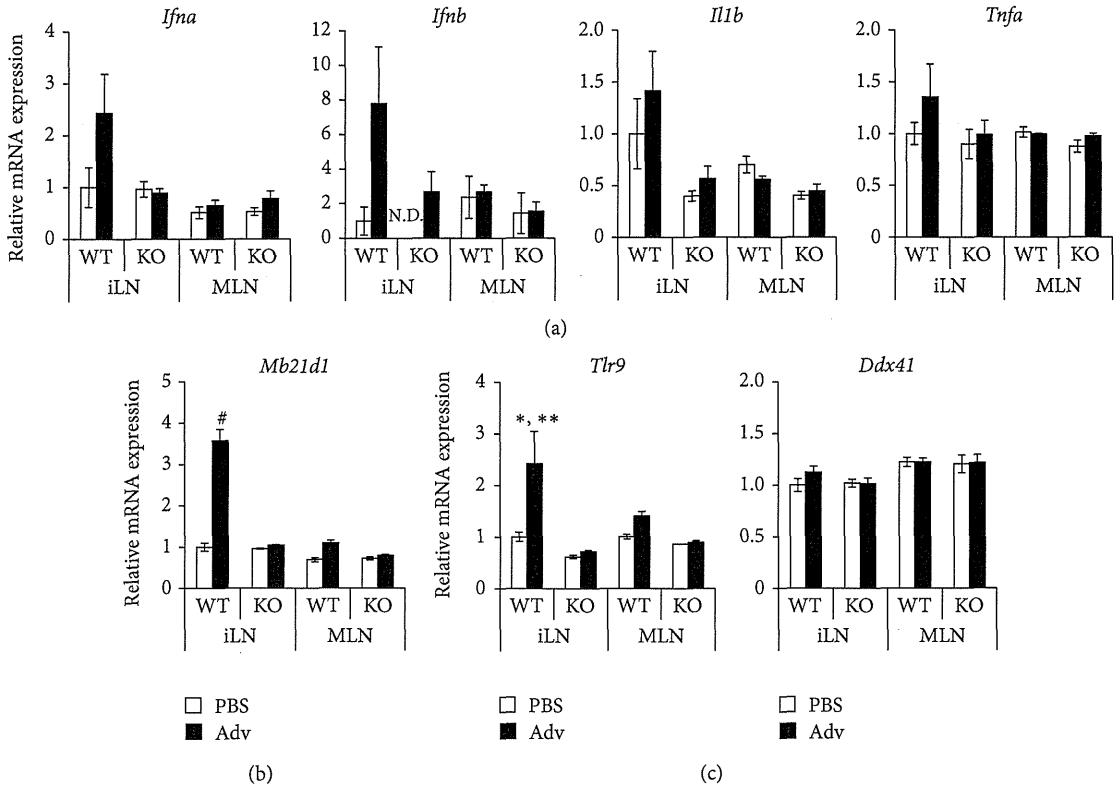

FIGURE 2: Relative mRNA expressions in the iLNs and MLN of WT and IFNAR2 KO mice following i.m. Adv vaccination. At 8 hours after the i.m. vaccination of 10^{10} vp of Ad-LacZ, total RNA was extracted from mononuclear cells in the LNs of each mouse. The mRNA expressions of *Ifna*, *Ifnb*, *Il1b*, *Tnfa* (a), *Mb21d1* (b), *Tlr9*, and *Ddx41* (c) in the LNs were measured by qRT-PCR, normalized by *Actb*. The graphs represent the relative mRNA expression of each gene normalized by that of PBS-administrated WT mice. Data are shown as the means ± S.E.M. ($n = 3$) and are representative of two independent experiments. $^{*}P < 0.05$ compared with other groups except for the MLN of Adv-administrated WT mice. $^{**}P < 0.01$ compared with the iLNs of IFNAR2 KO mice. $^{\#}P < 0.0001$ compared with other groups.

3.3. Type I IFN Signaling Is Required for the Early Activation of CTLs in iLNs. Since type I IFN signaling was not induced in IFNAR2 KO mice following i.m. Adv vaccination, we hypothesized that the early activation of T cells is not elicited sufficiently in IFNAR2 KO mice. After antigenic stimulation, T cells express a series of several activation markers, including CD69, CD44, and CD25, dependent on the developmental stages from naïve to effector. To examine whether the type I IFN signaling following i.m. Adv vaccination has an effect on an early activation marker, CD69 [27, 28], on $CD8^+$ T cells, we estimated the frequencies of $CD69^+$ cells in $CD8^+$ T cells residing in the DLNs. In Adv-administrated WT mice, the frequencies of $CD69^+$ cells in $CD8^+$ T cells in the iLNs were increased, while those in the MLN were not. However, in the case of Adv-administrated IFNAR2 KO mice, the frequencies of $CD69^+$ cells in $CD8^+$ T cells in the iLNs were significantly reduced compared with those of Adv-administrated WT mice (Figure 3). Thus, these data correlate with the results shown in Figure 2, in which the type I IFN response was elicited at the iLNs and diminished in IFNAR2 KO mice. These results indicated that type I IFN signaling induces the expression of CD69 on $CD8^+$ T cells in Adv-administrated mice. Collectively, these data suggest that the early activation of $CD8^+$ T cells via type I IFN signaling promotes the induction and/or migration of gut mucosal Ag-specific CTLs.

4. Discussion

In this study, we demonstrated that type I IFN signaling following i.m. Adv vaccination promotes the expression of IFN-α, IFN-β, and cGAS in the iLNs where Adv is mainly distributed at this time point and strongly induces the expression of CD69 on $CD8^+$ T cells in the iLNs. The expression of type I IFN is amplified through IFNAR [29, 30]. Therefore, it is reasonable that the expression of type I IFN is decreased in IFNAR2 KO mice. We observed that IFN-β expression was more strongly induced by type I IFN signaling than IFN-α expression. It has been reported that IFN-α is mainly produced by plasmacytoid dendritic cells (pDCs), while IFN-β is mainly produced by myeloid DCs (mDCs) and mouse embryonic fibroblasts (MEFs) [17, 31, 32]. Hence, it is speculated that type I IFN signaling contributes to IFN-β production from DCs and fibroblasts in the iLNs, such as stromal cells, following i.m. Adv vaccination. In addition, we observed a significant reduction in TLR9 expression as well as cGAS expression in IFNAR2 KO mice. cGAS and TLR9 have been reported to be the DNA sensors responsible for the

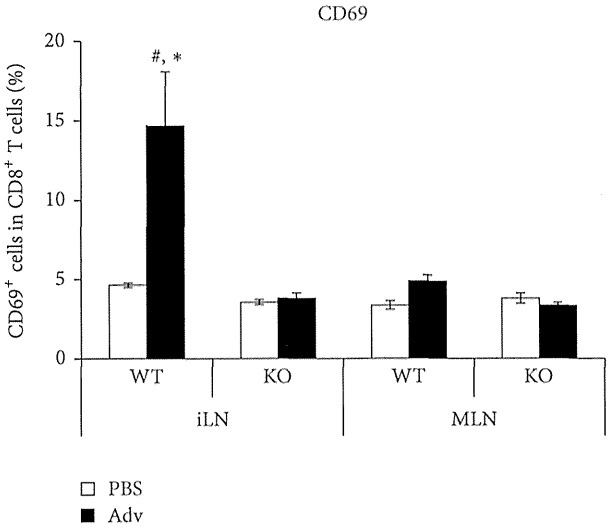

FIGURE 3: The frequencies of early activated $CD8^+$ T cells in the iLNs and MLN of WT and IFNAR2 KO mice following i.m. Adv vaccination. At 24 hours after the i.m. vaccination of 10^{10} vp of Ad-LacZ, the frequencies of $CD69^+$ T cells in $CD8^+$ T cells in the LNs of each mouse were measured by flow cytometry. Data are the pools of three independent experiments and are shown as the means ± S.E.M. ($n = 6$). $^*P < 0.001$ compared with the iLNs of PBS-administrated WT mice and MLN of Adv-administrated WT mice. $^\#P < 0.0001$ compared with other groups.

recognition of adenoviral DNA leading to the induction of type I IFN production [15, 16]. It is speculated that type I IFN signaling promotes the detection of Adv by cGAS and TLR9 and amplifies their signaling *in vivo*.

Recently, Weerd et al. revealed that IFN-β binds to the low-affinity component of IFNAR, IFNAR1, in the absence of IFNAR2 [33]. Moreover, IFNAR1-IFN-β complex activates unique intracellular signaling. However, in our study, we did not observe such phenomenon in IFNAR2 KO mice. For example, Weerd et al. showed that in IFNAR2 KO peritoneal exudate cells (PECs), IL-1β expression was upregulated 13.5-fold by IFN-β compared to nontreated IFNAR2 KO PECs. On the other hand, in our study, IL-1β expression in the iLNs of Adv-administrated IFNAR2 KO mice was upregulated just only 1.42-fold as much as that of PBS-administrated IFNAR2 KO mice (Figure 2(a)). Thus, it is speculated that the level of IFN-β in our study would be much lower than that in their study and the IFN-β signaling in our study would be transmitted via IFNAR2, which is the high-affinity component of IFNAR.

We observed a significant reduction of CD69 expression on $CD8^+$ T cells in the iLNs of IFNAR2 KO mice following i.m. Adv vaccination. Our results are consistent with a previous report that the expression of CD69 is strongly induced by type I IFN [34, 35]. CD69 inhibits egress of T cells from the spleen and secondary lymphoid tissues during T cell maturation [35]. It is speculated that the reduction of CD69 expression in IFNAR2 KO mice induces egress of $CD8^+$ T cells from the iLNs in the early stage of T cell maturation. In consequence, activated $CD8^+$ T cells in the iLNs fail to mature sufficiently, and thus, these cells do not acquire a gut-homing capacity. Moreover, Alari-Pahissa et al. recently reported that CD69 does not affect $CD8^+$ T cell priming following Ag-expressing vaccinia virus vector immunization [36]. Considering our previous finding that systemic Ag-specific CTLs are induced in IFNAR2 KO mice following i.m. Adv vaccination as similar as WT mice [8], it is likely that the reduction of CD69 expression on $CD8^+$ T cells does not alter $CD8^+$ T cell priming. For these reasons, it is suggested that type I IFN signaling-induced CD69 expression on $CD8^+$ T cells might regulate Ag-specific CTLs in the gut mucosal compartment.

In summary, we have shown the molecular mechanism of the induction of gut mucosal CTLs following i.m. Adv vaccination. We found that type I IFN signaling is required for the production of large amounts of type I IFN and the upregulation of CD69 on $CD8^+$ T cells in the iLNs. Our findings should contribute to the development of more efficient and safer mucosal vaccines and adjuvants.

Conflict of Interests

The authors declare that there is no conflict of interests regarding the publication of this paper.

Authors' Contribution

Masahisa Hemmi and Masashi Tachibana contributed equally to this paper.

Acknowledgment

This work was supported by grants from the Ministry of Health, Labour, and Welfare of Japan.

References

[1] J. Holmgren and C. Czerkinsky, "Mucosal immunity and vaccines," *Nature Medicine*, vol. 11, no. 4, pp. S45–S53, 2005.

[2] I. M. Belyakov and J. D. Ahlers, "Functional $CD8^+$ CTLs in mucosal sites and HIV infection: moving forward toward a mucosal AIDS vaccine," *Trends in Immunology*, vol. 29, no. 11, pp. 574–585, 2008.

[3] M. R. Neutra and P. A. Kozlowski, "Mucosal vaccines: the promise and the challenge," *Nature Reviews Immunology*, vol. 6, no. 2, pp. 148–158, 2006.

[4] N. Tatsis and H. C. J. Ertl, "Adenoviruses as vaccine vectors," *Molecular Therapy*, vol. 10, no. 4, pp. 616–629, 2004.

[5] D. R. Kaufman, J. Liu, A. Carville et al., "Trafficking of antigen-specific $CD8^+$ T lymphocytes to mucosal surfaces following intramuscular vaccination," *The Journal of Immunology*, vol. 181, no. 6, pp. 4188–4198, 2008.

[6] D. R. Kaufman, M. Bivas-Benita, N. L. Simmons, D. Miller, and D. H. Barouch, "Route of adenovirus-based HIV-1 vaccine delivery impacts the phenotype and trafficking of vaccine-elicited $CD8^+$ T lymphocytes," *Journal of Virology*, vol. 84, no. 12, pp. 5986–5996, 2010.

[7] S. Ganguly, S. Manicassamy, J. Blackwell, B. Pulendran, and R. R. Amara, "Adenovirus type 5 induces vitamin A-metabolizing

enzymes in dendritic cells and enhances priming of gut-homing CD8 T cells," *Mucosal Immunology*, vol. 4, no. 5, pp. 528–538, 2011.

[8] M. Shoji, M. Tachibana, K. Katayama et al., "Type-I IFN signaling is required for the induction of antigen-specific $CD8^+$ T cell responses by adenovirus vector vaccine in the gut-mucosa," *Biochemical and Biophysical Research Communications*, vol. 425, no. 1, pp. 89–93, 2012.

[9] T. Kawai and S. Akira, "Toll-like receptors and their crosstalk with other innate receptors in infection and immunity," *Immunity*, vol. 34, no. 5, pp. 637–650, 2011.

[10] O. Takeuchi and S. Akira, "Pattern recognition receptors and inflammation," *Cell*, vol. 140, no. 6, pp. 805–820, 2010.

[11] T. Kawai and S. Akira, "Innate immune recognition of viral infection," *Nature Immunology*, vol. 7, no. 2, pp. 131–137, 2006.

[12] B. Pulendran and R. Ahmed, "Translating innate immunity into immunological memory: implications for vaccine development," *Cell*, vol. 124, no. 4, pp. 849–863, 2006.

[13] Z. C. Hartman, A. Kiang, R. S. Everett et al., "Adenovirus infection triggers a rapid, MyD88-regulated transcriptome response critical to acute-phase and adaptive immune responses in vivo," *Journal of Virology*, vol. 81, no. 4, pp. 1796–1812, 2007.

[14] J. Zhu, X. Huang, and Y. Yang, "Innate immune response to adenoviral vectors is mediated by both Toll-like receptor-dependent and -independent pathways," *Journal of Virology*, vol. 81, no. 7, pp. 3170–3180, 2007.

[15] T. Yamaguchi, K. Kawabata, N. Koizumi et al., "Role of MyD88 and TLR9 in the innate immune response elicited by serotype 5 adenoviral vectors," *Human Gene Therapy*, vol. 18, no. 8, pp. 753–762, 2007.

[16] E. Lam, S. Stein, and E. Falck-Pedersen, "Adenovirus detection by the cGAS/STING/TBK1 DNA sensing cascade," *Journal of Virology*, vol. 88, no. 2, pp. 974–981, 2014.

[17] T. Yamaguchi, K. Kawabata, E. Kouyama et al., "Induction of type I interferon by adenovirus-encoded small RNAs," *Proceedings of the National Academy of Sciences of the United States of America*, vol. 107, no. 40, pp. 17286–17291, 2010.

[18] S. E. Hensley, W. Giles-Davis, K. C. McCoy, W. Weninger, and H. C. J. Ertl, "Dendritic cell maturation, but not $CD8^+$ T cell induction, is dependent on type I IFN signaling during vaccination with adenovirus vectors," *The Journal of Immunology*, vol. 175, no. 9, pp. 6032–6041, 2005.

[19] S. N. Mueller and R. N. Germain, "Stromal cell contributions to the homeostasis and functionality of the immune system," *Nature Reviews Immunology*, vol. 9, no. 9, pp. 618–629, 2009.

[20] M. Perreau, H. C. Welles, C. Pellaton et al., "The number of toll-like receptor 9-agonist motifs in the adenovirus genome correlates with induction of dendritic cell maturation by adenovirus immune complexes," *Journal of Virology*, vol. 86, no. 11, pp. 6279–6285, 2012.

[21] K. J. Ishii, T. Kawagoe, S. Koyama et al., "TANK-binding kinase-1 delineates innate and adaptive immune responses to DNA vaccines," *Nature*, vol. 451, no. 7179, pp. 725–729, 2008.

[22] K. Kawabata, F. Sakurai, T. Yamaguchi, T. Hayakawa, and H. Mizuguchi, "Efficient gene transfer into mouse embryonic stem cells with adenovirus vectors," *Molecular Therapy*, vol. 12, no. 3, pp. 547–554, 2005.

[23] N. Hitoshi, Y. Ken-ichi, and M. Jun-ichi, "Efficient selection for high-expression transfectants with a novel eukaryotic vector," *Gene*, vol. 108, no. 2, pp. 193–199, 1991.

[24] J. V. Maizel Jr., D. O. White, and M. D. Scharff, "The polypeptides of adenovirus. I. Evidence for multiple protein components in the virion and a comparison of types 2, 7A, and 12," *Virology*, vol. 36, no. 1, pp. 115–125, 1968.

[25] J. W. Schoggins, S. J. Wilson, M. Panis et al., "A diverse range of gene products are effectors of the type I interferon antiviral response," *Nature*, vol. 472, no. 7344, pp. 481–485, 2011.

[26] Z. Zhang, B. Yuan, M. Bao, N. Lu, T. Kim, and Y.-J. Liu, "The helicase DDX41 senses intracellular DNA mediated by the adaptor STING in dendritic cells," *Nature Immunology*, vol. 12, no. 10, pp. 959–965, 2011.

[27] J. F. Krowka, B. Cuevas, D. C. Maron, K. S. Steimer, M. S. Ascher, and H. W. Sheppard, "Expression of CD69 after in vitro stimulation: a rapid method for quantitating impaired lymphocyte responses in HIV-infected individuals," *Journal of Acquired Immune Deficiency Syndromes and Human Retrovirology*, vol. 11, no. 1, pp. 95–104, 1996.

[28] P. E. Simms and T. M. Ellis, "Utility of flow cytometric detection of CD69 expression as a rapid method for determining poly- and oligoclonal lymphocyte activation," *Clinical and Diagnostic Laboratory Immunology*, vol. 3, no. 3, pp. 301–304, 1996.

[29] I. Marié, J. E. Durbin, and D. E. Levy, "Differential viral induction of distinct interferon-α genes by positive feedback through interferon regulatory factor-7," *The EMBO Journal*, vol. 17, no. 22, pp. 6660–6669, 1998.

[30] M. Dalod, T. Hamilton, R. Salomon et al., "Dendritic cell responses to early murine cytomegalovirus infection: subset functional specialization and differential regulation by interferon α/β," *The Journal of Experimental Medicine*, vol. 197, no. 7, pp. 885–898, 2003.

[31] E. Basner-Tschakarjan, E. Gaffal, M. O'Keeffe et al., "Adenovirus efficiently transduces plasmacytoid dendritic cells resulting in TLR9-dependent maturation and IFN-α production," *Journal of Gene Medicine*, vol. 8, no. 11, pp. 1300–1306, 2006.

[32] G. Fejer, L. Drechsel, J. Liese et al., "Key role of splenic myeloid DCs in the IFN-$\alpha\beta$ response to adenoviruses in Vivo," *PLoS Pathogens*, vol. 4, no. 11, Article ID e1000208, 2008.

[33] N. A. de Weerd, J. P. Vivian, T. K. Nguyen et al., "Structural basis of a unique interferon-β signaling axis mediated via the receptor IFNAR1," *Nature Immunology*, vol. 14, no. 9, pp. 901–907, 2013.

[34] K. Radulovic, C. Manta, V. Rossini et al., "CD69 regulates type I IFN-induced tolerogenic signals to mucosal CD4 T cells that attenuate their colitogenic potential," *The Journal of Immunology*, vol. 188, no. 4, pp. 2001–2013, 2012.

[35] L. R. Shiow, D. B. Rosen, N. Brdičková et al., "CD69 acts downstream of interferon-α/β to inhibit S1P 1 and lymphocyte egress from lymphoid organs," *Nature*, vol. 440, no. 7083, pp. 540–544, 2006.

[36] E. Alari-Pahissa, L. Notario, E. Lorente et al., "CD69 does not affect the extent of T cell priming," *PLoS ONE*, vol. 7, no. 10, Article ID e48593, 2012.

OPEN ACCESS Freely available online

PLOS ONE

Protective Epitopes of the *Plasmodium falciparum* SERA5 Malaria Vaccine Reside in Intrinsically Unstructured N-Terminal Repetitive Sequences

Masanori Yagi[1☯], Gilles Bang[2☯], Takahiro Tougan[1], Nirianne M. Q. Palacpac[1], Nobuko Arisue[1], Taiki Aoshi[3,4], Yoshitsugu Matsumoto[5], Ken J. Ishii[3,4], Thomas G. Egwang[6], Pierre Druilhe[2¤], Toshihiro Horii[1]*

1 Department of Molecular Protozoology, Research Institute for Microbial Diseases, Osaka University, Suita, Osaka, Japan, **2** Laboratoire de Parasitologie Bio-Médicale, Institut Pasteur, Paris, France, **3** Laboratory of Adjuvant Innovation, National Institute of Biomedical Innovation, Ibaraki, Osaka, Japan, **4** Laboratory of Vaccine Science, Immunology Frontier Research Center, Osaka University, Suita, Osaka, Japan, **5** Laboratory of Molecular Immunology, School of Agriculture and Life Sciences, The University of Tokyo, Tokyo, Japan, **6** Med Biotech Laboratories, Kampala, Uganda

Abstract

The malaria vaccine candidate antigen, SE36, is based on the N-terminal 47 kDa domain of *Plasmodium falciparum* serine repeat antigen 5 (SERA5). In epidemiological studies, we have previously shown the inhibitory effects of SE36 specific antibodies on *in vitro* parasite growth and the negative correlation between antibody level and malaria symptoms. A phase 1 b trial of the BK-SE36 vaccine in Uganda elicited 72% protective efficacy against symptomatic malaria in children aged 6–20 years during the follow-up period 130–365 days post–second vaccination. Here, we performed epitope mapping with synthetic peptides covering the whole sequence of SE36 to identify and map dominant epitopes in Ugandan adult serum presumed to have clinical immunity to *P. falciparum* malaria. High titer sera from the Ugandan adults predominantly reacted with peptides corresponding to two successive N-terminal regions of SERA5 containing octamer repeats and serine rich sequences, regions of SERA5 that were previously reported to have limited polymorphism. Affinity purified antibodies specifically recognizing the octamer repeats and serine rich sequences exhibited a high antibody-dependent cellular inhibition (ADCI) activity that inhibited parasite growth. Furthermore, protein structure predictions and structural analysis of SE36 using spectroscopic methods indicated that N-terminal regions possessing inhibitory epitopes are intrinsically unstructured. Collectively, these results suggest that strict tertiary structure of SE36 epitopes is not required to elicit protective antibodies in naturally immune Ugandan adults.

Citation: Yagi M, Bang G, Tougan T, Palacpac NMQ, Arisue N, et al. (2014) Protective Epitopes of the *Plasmodium falciparum* SERA5 Malaria Vaccine Reside in Intrinsically Unstructured N-Terminal Repetitive Sequences. PLoS ONE 9(6): e98460. doi:10.1371/journal.pone.0098460

Editor: Georges Snounou, Université Pierre et Marie Curie, France

Received January 24, 2014; **Accepted** May 4, 2014; **Published** June 2, 2014

Funding: This work was supported by Grant-in-Aid for Young Scientists (B) (22770151) and Grant-in-Aid for Global COE (Centers of Excellence) Program to MY; Grant-in-Aid for Scientific Research (A) (24249024), Program for the Promotion of International Policy Dialogues Contributing to the Development of Science and Technology Diplomacy to TH from the Japanese Ministry of Education, Science, Sports, Culture and Technology. The authors would like to acknowledge the funding support of Global Health Innovative Technology Fund (GHIT RFP 2013-001) to TH under the project Clinical development of BK-SE36/CpG malaria vaccine. The funders had no role in the study design, data collection and analysis, decision to publish, or preparation of the manuscript.

Competing Interests: The authors have declared that no competing interests exist.

* E-mail: horii@biken.osaka-u.ac.jp

☯ These authors contributed equally to this work.

¤ Current address: The Vac4all initiative, Paris, France

Introduction

Despite the vast malaria burden no effective malaria vaccine exists [1,2]. The development of malaria vaccines has mainly focused on *Plasmodium falciparum*, the most deadly of five *Plasmodium* species that infect humans. Malaria vaccine development strategies vary depending on the target stages of the parasite life cycle, i.e. sporozoite, intra-hepatocytic stage, asexual erythrocyte stages, gametocyte, and mosquito midgut stages. Asexual erythrocyte stage antigens are thought to elicit antibodies which reduce blood parasitemia and lessen the severity of malaria symptoms. However, sequence polymorphism of many antigens, as observed in several vaccine candidates such as merozoite surface protein (MSP)-1, MSP-2 [3] and apical membrane antigen-1 (AMA-1) [4], hamper the systematic vaccine development strategy based on host immune responses against malaria parasites.

P. falciparum serine repeat antigen 5 (*Pf*SERA5) is one of the candidate vaccines in human trial [5–7]. Abundantly expressed in the parasitophorous vacuole and on the merozoite surface, and belonging to the SERA protein family, the 120 kDa protein is processed into 47, 50, 6 and 18 kDa domains at the time of schizont rupture. While the 50 and 6 kDa domains are secreted, the 47 and 18 kDa domains are covalently linked by disulfide bond(s) and remain on the merozoite surface [7–9]. *Pf*SERA5 was the first physiological substrate identified for *P. falciparum* subtilisin-like serine protease (*Pf*SUB1) [10].

Sequence analysis of 445 *P. falciparum* field isolates from nine countries worldwide revealed that sequence polymorphism of

*Pf*SERA5 is remarkably limited unlike other malaria vaccine candidates [11]. Moreover, high antibody level against the N-terminal 47 kDa domain correlated with the absence of fever or low parasitemia [5,12,13]. Under *in vitro* conditions, antibodies against the N-terminal domain were also suggested to correlate with antiparasitic effects through several mechanisms. At high antibody concentration, inhibition of parasite growth was found to be associated with merozoite agglutination [14] or complement mediated cell lysis of segmented schizont [15]. At low antibody concentrations, monocyte-mediated antibody dependent cellular inhibition (ADCI) activity has been demonstrated [16].

SE36 is based on the N-terminal 47 kDa domain constructed by removing the polyserine region located in the middle of the domain [5]. A recent phase 1 b clinical trial and follow-up study 365 days post-second vaccination elicited 72% protective efficacy against symptomatic malaria in Ugandan children aged 6–20 years [6]. Although the exact function of *Pf*SERA5 remains unknown, a parasite inhibitory epitope defined by a murine monoclonal antibody was mapped onto amino acids 17–73 of the Honduras-1 strain, a well conserved region in diverse geographical isolates of *P. falciparum* [17,18].

Intrinsically unstructured proteins (IUPs), also called intrinsically disordered proteins or natively unfolded proteins, have for the past 10–20 years generated interest because of their unusual way to carry out molecular recognition different from traditional protein structure-function paradigms. IUPs contain polypeptide chains lacking stable tertiary structure when they exist alone, however, some of them are known to switch to more ordered conformation upon recognition of their binding partners and play their biological roles [19,20].

*Pf*SERA5 (17–73) has an octamer repeat (OR) region and a serine rich (SR) region. The repeat number of octamer motifs varies depending on strains but the basic motif sequences are well conserved in *P. falciparum* [11]. These OR and SR regions have biased amino acid composition and are low complexity regions with little diversity in their amino acids [21]. Low complexity regions are often found in *Plasmodium* species and, due to lack of hydrophobic amino acids, such regions are expected to be intrinsically unstructured [22]. *P. falciparum* proteins, such as MSP-2 and trophozoite exported protein 1 (Tex1), are reported to have intrinsically unstructured regions (IURs) [23–25]. P27A, an IUR found in Tex-1, was well recognized by sera from individuals living in malaria endemic areas. Moreover, murine antibodies purified from P27A immunized mice showed high ADCI activities [24]. Immunogenicity of IUR in naturally infected humans was also reported for *P. vivax* AMA-1 [26].

In the present study, we performed epitope mapping with overlapping synthetic peptides covering the whole sequence of SE36 utilizing serum from Ugandan volunteers, and serum from previously vaccinated mice and squirrel monkeys. We identified the N-terminal repetitive sequence regions of SE36 as immunodominant IgG epitopes in Ugandan individuals presumed to have clinical immunity to *P. falciparum* malaria. We have demonstrated previously that antibodies raised against N-terminal region of *Pf*SERA5 strongly inhibit *in vitro* parasite growth by ADCI at concentrations which do not show any detectable direct inhibition of growth [16], thus we used this assay as a screen for functional inhibition activity of anti-SE36 IgG. Affinity purified antibodies against N-terminal repetitive sequence regions of SE36 showed high ADCI activities suggesting that the regions are protective epitopes. Additionally, the OR and SR regions are revealed to be intrinsically unstructured by spectroscopic methods and protein structure predictions. These results show that the N-terminal repetitive sequences have characteristics of an intrinsically unstructured region and are highly immunogenic in Ugandan adults eliciting protective antibodies against malaria.

Materials and Methods

Ethics Statement

Serum samples from pool of individuals living in endemic areas and individual Ugandan serum samples were from participants in an earlier epidemiological study [9]. Briefly, the study utilizes residual samples from a cross-sectional study of 40 (37 sera are available for this study) healthy Ugandan adults living in Atopi Parish, a malaria holoendemic area, located 5 km west of Apac Town, 300 km north of Kampala. Ethical clearance for sampling and consent was obtained and approved by the Uganda National Council for Science and Technology under the 1997 Guidelines for Health Research Involving Human Subjects in Uganda [9]. In agreement with the local community leadership, a process of dialogue was done. Information about the study was given to the head of the community, household and study participants. Verbal consent was obtained for voluntary participation and for blood samples to be taken and stored for use in future studies. It was deemed culturally-sensitive in this community that experienced recent government conflict that verbal informed consent be sought (written consent were not practiced, disliked and viewed as mistrust). Being a cross-sectional study, signatures will also be the only record of their participation and risk of privacy is minimized if their signature is not recorded. No other records exist for their participation. Blood samples were coded during blood collection, processed within a few hours after collection and separated into sera, which was stored at −20°C and −70°C until analyses.

Animal housing, care and handling of squirrel monkeys were done in strict compliance with "The guidelines for the care and use of laboratory animals" by the University of Tokyo [5]. Briefly, male squirrel monkeys (*Saimiri sciureus*) of Guyana phenotype were bred in captivity. The monkeys were quarantined and conditioned for at least a month prior to the commencement of the study. Thorough medical examinations revealed that the animals were free of all intestinal and any blood stage infections including malaria, and they were declared to be in a general good health by a veterinarian. They were housed in the Amami Laboratory of Injurious Animals, Institute of Medical Science, University of Tokyo in individual safety cabinets with an exercise bar at a controlled environment of 24±2°C and 50±10% humidity. Monkeys were fed with new world monkey chow (Clea Japan Inc., Tokyo, Japan) and allowed free access to water. Lighting was automatically regulated on a 12 hours light-dark cycle. The monkeys, weighing between 680 and 760 g at the beginning of the experiment, were divided into two treatment groups that received their intramuscular injection on the left thigh 5 and 3 weeks before challenge infection. All procedures were performed under anesthesia and all efforts were made to minimize suffering. All experimental procedures were approved by the School of Agriculture and Life Sciences, the University of Tokyo. Additional details of animal welfare/care and steps taken to ameliorate suffering were in accordance with the recommendations of the Weatherall report, "The use of non-human primates in research". During the study no monkey died or was sacrificed.

Animal experiments using mice were approved by the Animal Care and Use Committee of the Research Institute for Microbial Diseases, Osaka University, Japan. Mice care and steps to ameliorate suffering was conducted in accordance with the guidelines of the committee and immunization experiments were in accordance with the GERBU adjuvant protocol described

below (GERBU Biotechnik GmbH, Heidelberg, Germany). During the study, no mice were sacrificed.

Animal Blood Samples

Residual serum samples from squirrel monkeys (*Saimiri sciureus*) that received 50 µg SE36 protein with 500 µg aluminum hydroxide gel in 0.5 ml of PBS and those in the control group that received the same volume of PBS by intra-muscular injection were utilized [5]. In brief, after 2 or 3 immunizations, these monkeys were followed through after *P. falciparum* challenge infection [5]. For mouse immunization, 30 ddY mice were purchased from Japan SLC, Inc. (Hamamatsu, Japan). Each mouse was subcutaneously immunized with 50 µl of 1 mg/ml SE36 protein and 50 µl GERBU adjuvant (100 µl in total) 4 times at 2-week intervals. Two weeks after last immunization, blood draw was performed from the mouse tail and blood samples from the mice were pooled for the experiments.

Recombinant SE36 Protein

GMP grade SE36 protein was expressed in *E. coli* using a codon optimized synthetic gene and purified as previously described [5].

Synthetic Peptides

Fifteen synthetic peptides of 40–42 residues covering the whole sequence of SE36 protein were synthesized by Operon Biotechnology Inc. (Tokyo, Japan) (Fig. 1 and Table S1, series I). Each peptide was designed to overlap with two adjacent peptides at its N- and C-terminal halves, respectively.

Enzyme-Linked Immunosorbent Assay

Enzyme-linked immunosorbent assay (ELISA) was performed using flat-bottomed 96-well Nunc-Immuno plates (Nunc, Roskilde, Denmark). SE36 protein or the synthetic peptides were dissolved in carbonate buffer (pH 9.6) as coating buffer at a concentration of 0.1 µg/ml. For ELISA assays of synthetic peptides, each plate was coated with the whole peptide series. The plates were coated overnight at 4°C with 100 µl of the protein or peptide solutions, washed three times with PBS containing 0.05% Tween 20 (PBS/T) and blocked for an hour with 5% skim milk in PBS at 37°C. The plates were again washed three times with PBS/T prior to addition of serum samples or purified IgG prepared in 5% skim milk in PBS/T. Test samples were added to wells at optimized concentration and incubated for an hour at 37°C. After washing with PBS/T, peroxidase-conjugated goat IgG fraction to human IgG (whole molecule) (55220; Cappel ICN Pharmaceuticals Inc, Aurora, OH) diluted 1:2000; or horseradish peroxidase-conjugated rabbit anti-human IgG antibody (A8792; Sigma-Aldrich Corp., St. Louis, MO) diluted 1:2000; or peroxidase conjugated affiniPure goat anti-mouse IgG antibody (H+L) (115-035-166; Jackson ImmunoResearch Laboratories, Inc., West Grove, PA) diluted 1:5000 in 5% skim milk in PBS/T was added to the plates and incubated at 37°C for 1 hour. The plates were washed and incubated with 100 µl freshly prepared citrate-phosphate buffer (pH 5.0) containing 0.2% hydrogen peroxide and OPD tablet (154-01673; Sigma-Aldrich Corp., St. Louis, MO) for 15 minutes. The reaction was stopped with 100 µl of 2 M sulfuric acid and optical density was read at 492 nm.

Purification of Antibodies

To prepare anti-OR and anti-SR antibodies for ADCI experiments, the antibodies were purified from Ugandan high antibody titer serum pool (SE36-positive serum pool) [9]. Prior to the purification of antibodies specific to the OR or SR region, whole antibodies were purified from the serum pool with HiTrap Protein G HP columns (GE Healthcare UK Ltd, Buckinghamshire, UK). Antibodies purified by Protein G columns were then loaded to either OR or SR-specific peptide columns. The OR/SR peptide columns were prepared with SulfoLink Immobilization Kit for Peptides (Thermo Fisher Scientific, Waltham, MA), so that OR/SR peptides with cysteine residues at the N-termini (series II peptides 1 and 3, Table S2) were immobilized to the columns via thiol groups, following recommendations of the manufacturer. Antibodies bound to the columns were eluted with 0.1 M Gly-HCl at pH 2.7 and immediately neutralized with 1 M Tris-HCl at pH 8.5.

Murine serum pool from SE36-vaccinated mice was used to purify the antibody against the whole SE36 molecule. However, due to limited sample volume, after applying to Protein G column no further purification was done. All antibodies were dialyzed against RPMI 1640 (Nakalai Tesque, Kyoto, Japan) prior to ADCI assays.

Antibody-Dependent Cellular Inhibition Assay (ADCI) and Assessment of Parasitemia by Flow Cytometry

The ADCI assay was as previously described [27,28] and carried out with either (i) human IgG purified with protein G and then affinity purified for specific peptides; or (ii) protein G purified IgG from mice immunized with SE36. Final concentration of IgG was at 0.3 mg/ml. As a positive control, a pool of hyperimmune African adults IgG (PIAG) [27] was used at 2 mg/ml to assess reproducibility between each assay. Monocytes (MN) from peripheral blood mononuclear cells were further enriched using EasySep Human Monocyte Enrichment Kit Without CD16 Depletion according to manufacturer's instruction (StemCell Technologies Inc., Vancouver, BC, Canada). Monocyte monolayer was obtained after incubation of 2×10^5 MN for 30 minutes at 37°C in 5% CO_2 atmosphere. A synchronized asexual blood stage parasite culture (K1 clone) with very mature schizonts (0.5% parasitemia, 2.5% haematocrit) was added on the MN monolayer in addition to murine and human IgG to be tested. Intrinsic antiparasitic effect of control and test IgG sera was assessed in wells containing the blood stage parasites without MN. Prior to ADCI assay, only MN with non-significant phagocytosis effect against *in vitro* growth of asexual blood stage parasites were selected. Samples were tested in duplicate wells. Plates were incubated in a candle jar

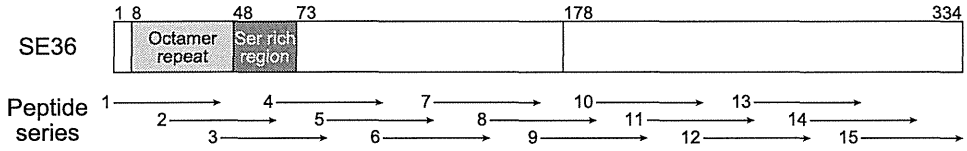

Figure 1. Schematic representation of synthetic peptide series I covering the whole sequence of SE36 protein. The number 178 denotes the position of polyserine sequence present in *Pf*SERA5 but deleted in SE36 [5].
doi:10.1371/journal.pone.0098460.g001

at 37°C, in a 5% CO_2 incubator. At 48 and 72 hours, 50 µl of complete medium was added to each well. At 96 hours the assay was stopped and the parasitemia determined by flow cytometry (FACSCalibur, BD Biosciences, CA). Assays were performed at the same day by two independent researchers.

Flow cytometry enumeration of infected erythrocytes with viable malaria parasites was performed by double staining of DNA and RNA using hydroethidine (HE) and thiazole orange (TO) (Sigma-Aldrich Corp.). Briefly, erythrocytes were incubated for 20 min at 37°C in the dark with 20 µg/ml of HE diluted in PBS-1% FCS (FACS buffer), washed three times in FACS buffer, followed by another incubation for 30 min at room temperature in the dark with TO diluted at 1:15000 in FACS buffer. Analysis was performed on 1×10^5 erythrocytes with the CellQuest Pro software. Parasitemia was determined as the percentage of double stained infected erythrocytes among the whole erythrocyte population. The specific growth inhibitory index (SGI) was calculated according to the following formula: SGI = 100×[1-(percent parasitemia with MN and test IgG/percent parasitemia with test IgG)/(percent parasitemia with MN and naïve IgG/percent parasitemia with naïve IgG)]. An SGI effect was considered as significant if yielding a value >30% [29].

Protein Structure Prediction

The amino acid sequences of the N-terminal domains of *Pf*SERA1-9 (3D7) were aligned with Multiple Sequence Alignment Tool version 1.1 (http://cib.cf.ocha.ac.jp/KYG/onlyalign.html) [30] after deletion of N-terminal signal sequences predicted by SignalP 3.0 [31]. Since *Pf*SERA8 has no corresponding region, amino acid sequence identity and similarity of relatively conserved regions among *Pf*SERA1-7 and 9 were calculated based on Clustal W alignment and similarity classification in NPS@server (http://npsa-pbil.ibcp.fr/) [32,33]. Percentage "identity" and "strong similarity" were calculated from the sum of the number of amino acids (Table 1). For prediction of disordered/ordered structure, the sequences were applied to Consensus Disorder Prediction (http://protease.burnham.org/www/tools/html/disorder.html) [34]. Secondary structure prediction of SE36 was performed by Consensus secondary structure prediction in NPS@ server [33].

Circular Dichroism

Circular dichroism (CD) spectra were acquired with a J-820 spectropolarimeter (Jasco, Tokyo, Japan) at 5–37°C. Samples were prepared at 0.2 mg/ml for SE36 or 0.1 mg/ml for peptides in 50 mM sodium phosphate and 150 mM NaCl with or without 40% 2,2,2-trifluoroethanol (TFE). Each spectrum is an average of 20–40 times measurements. The obtained data were converted into mean residue ellipticity, [θ]. Peptide concentrations were determined using BCA Protein Assay Kit (Thermo Fisher Scientific). For SE36, the concentration was determined from absorbance at 280 nm using an extinction coefficient calculated as reported by Gill and von Hippel [5,35].

Tryptophan Fluorescence

Tryptophan fluorescence spectra were acquired with a F-7000 fluorescence spectrophotometer (Hitachi, Tokyo, Japan) at 25°C with excitation wavelength at 295 nm and emission detection wavelength between 300 to 450 nm. Samples were prepared at 0.2 mg/ml in 50 mM sodium phosphate and 150 mM NaCl with or without 8 M urea.

Table 1. Amino acid sequence identity and similarity of the relatively conserved regions (brown bars in Fig. 5) in the N-terminal domain between SE36 (Honduras-1 SERA5) and 3D7 SERA proteins.

3D7 SERA	1	2	3	4	5	6	7	9
Identity (%)	57.2	50.7	54.6	51.3	98.0	53.9	50.7	52.0
Similarity (%)	80.9	77.0	80.9	77.0	99.3	74.3	78.3	80.3

doi:10.1371/journal.pone.0098460.t001

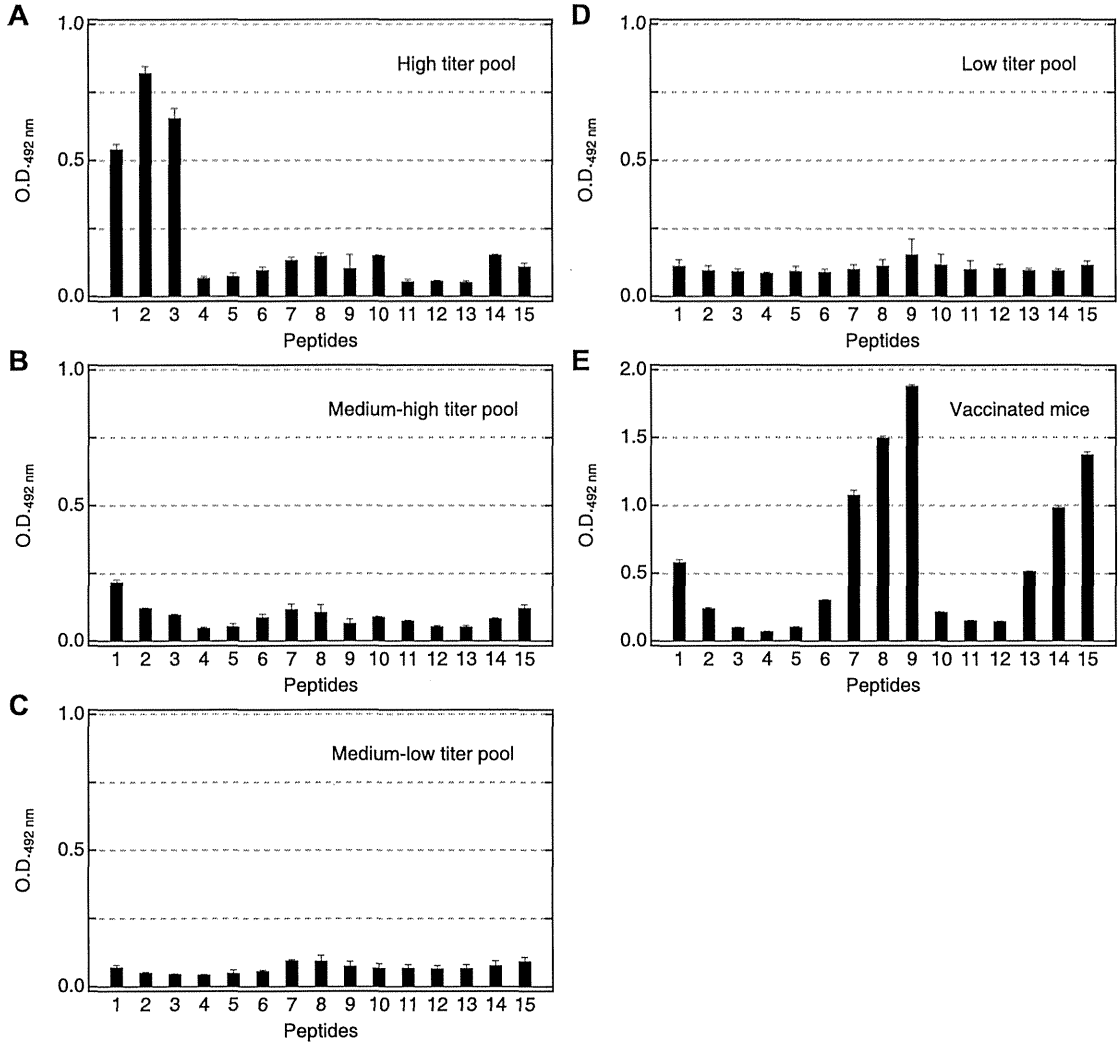

Figure 2. Reactivity of pooled Ugandan serum samples and a vaccinated mouse serum pool against synthetic peptide series I. (**A**) High, (**B**) medium-high, (**C**) medium-low, (**D**) low titer sera pool. Each pool consists of equal aliquots of 9–10 individual sera. The geometric mean anti-SE36 IgG titers of the individual samples are in Table S2. The patterns of reactivity for 18 individual sera are shown in Fig. S2. Serum samples were diluted 800-fold. Secondary antibody was peroxidase-conjugated goat IgG fraction to human IgG (whole molecule) (55220; Cappel ICN Pharmaceuticals Inc, Aurora, OH) diluted 1:2000. (**E**) Pooled serum from five mice used at 1:1,600. Secondary antibody was peroxidase conjugated affiniPure goat anti-mouse IgG antibody (H+L) (115-035-166; Jackson ImmunoResearch Laboratories, Inc., West Grove, PA) diluted 1:5000. All sera were tested for ELISA at least four times. Error bars reflect standard deviation. Reactivity of malaria naïve Japanese serum and naïve mouse serum are shown in Fig. S2.
doi:10.1371/journal.pone.0098460.g002

Results

Reactivity of Anti-SE36 Positive Ugandan Serum against the Synthetic Peptides

To determine antigenic regions of SE36, overlapping synthetic peptides corresponding to the N-terminal domain of *Pf*SERA5 (Honduras-1) were prepared (Fig. 1). Based on anti-SE36 IgG levels (Table S2), four pools of high (9 individuals), medium-high (9 individuals), medium-low (9 individuals) and low (10 individuals) titer sera were made and tested for reactivity with peptide series I (Details are in Table S1). As shown in Fig. 2A, pooled high titer sera predominantly reacted with peptides 1, 2 and 3. Peptides 1–3 correspond to the OR and SR regions. Looking at individual sera, more than half of the individuals in the high titer group (or those presumed to have clinical immunity to *P. falciparum* infection) predominantly reacted with peptides 1, 2 and/or 3 (Fig. S2A–D, F, G, I). Medium and low titer pooled sera (Fig. 2B–D), as well as the Japanese naïve control serum (Fig. S2S), reacted poorly to these peptides. In addition, two randomly chosen high titer Ugandan serum samples (PRI and T69) were also examined with another overlapping peptide set (Table S1, series II) which had a different span in the SE36 protein (Fig. S1A, a set of 26 peptides with 20–40 residues). Again, both high titer sera predominantly reacted with peptides 1 and 2, with Ugandan T69 serum also

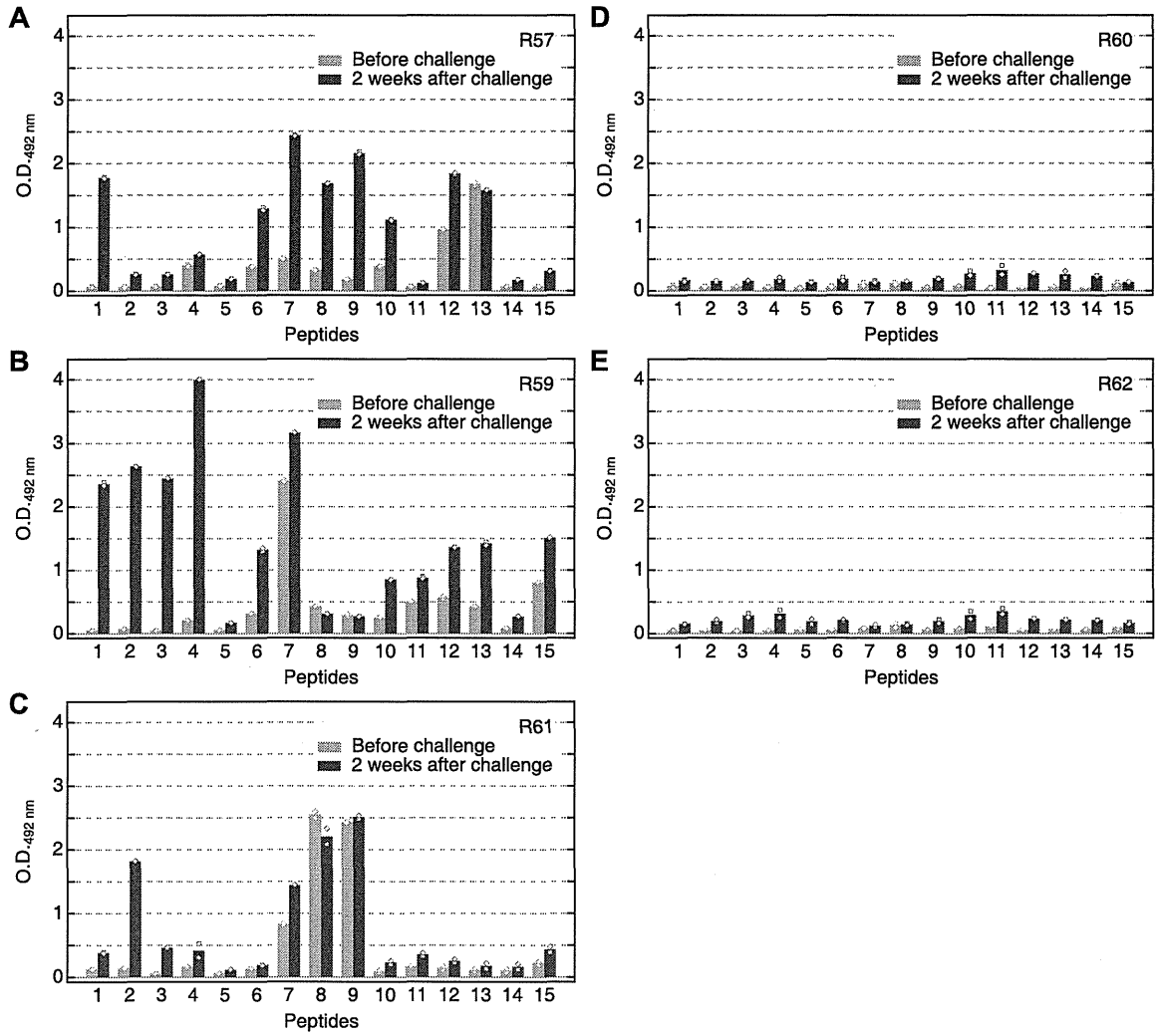

Figure 3. Reactivity in squirrel monkeys. The reactivity of the serum samples from vaccinated (**A–C**) and non-vaccinated (**D, E**) squirrel monkeys against the different peptides in Fig. 1 and Table S1 series I. Red and green bars represent samples before challenge infection and two weeks after challenge infection, respectively. R57, R59-62 are subject codes for squirrel monkeys. Monkey serum were diluted 1:400; secondary antibody was horseradish peroxidase-conjugated rabbit anti-human IgG antibody (A8792; Sigma-Aldrich Corp., St. Louis, MO) diluted 1:2000. Mean values from duplicate ELISA with individual data points are shown.
doi:10.1371/journal.pone.0098460.g003

showing reactivity to peptide 3 (Fig. S1B–1 and B–2). This is in contrast to an SE36 vaccinated mouse serum pool that reacted broadly with a number of regions/peptides as shown in Fig. 2E. Reactivity to naïve mouse serum is shown in Fig. S2T.

From Ugandan serum reactivity, it appears that the OR and SR repetitive sequences in the N-terminal regions are highly antigenic in Ugandan adults with high anti-SE36 antibody titers.

Reactivity of Vaccinated Squirrel Monkey Serum against the Synthetic Peptides

We performed epitope mapping using serum samples obtained previously from SE36 vaccinated squirrel monkeys. Sera from those monkeys vaccinated with SE36 before and after *P. falciparum* challenge infection were used. Before challenge infection, the spectra of reactivity against the peptides were broad, similar to vaccinated mouse serum pool. After challenge infection, some reactivity was observed to the peptides corresponding to OR and SR sequences (Fig. 3A–C). In contrast, monkeys in the control group (without SE36 vaccination) did not show marked response to the synthetic peptides even after challenge infection (Fig. 3D, E). Thus, as earlier reported [5], without SE36 vaccination, no anti-SE36 antibody can be induced despite challenge infection. However, priming the host with SE36 vaccination resulted in a boosting of immune response at the OR and SR sequences by challenge infection. We cannot exclude the presence of other protective epitopes outside the OR and SR sequences (located downstream of the OR and SR sequences) since we did not observe dominant reactivity against OR and/or SR sequences yet all three vaccinated squirrel monkeys were protected from high parasitemia [5].

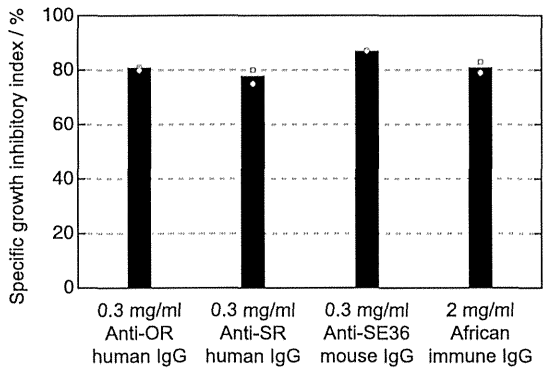

Figure 4. Antibody-dependent cellular inhibition activity with affinity purified antibodies. *In vitro* parasite specific growth inhibition (SGI) in the presence of human monocytes and human affinity-purified anti-OR or anti-SR IgG or murine anti-SE36 IgG at 0.3 mg/ml. A pool of polyclonal immune African IgG from individuals living in endemic areas was used as positive control at a final concentration of 2 mg/ml. IgG purified from malaria naïve human sera was used as negative control and included in the formula for SGI calculation as described in Materials and Methods. Mean values from duplicate ELISA with individual data points are shown.
doi:10.1371/journal.pone.0098460.g004

Antibody-Dependent Cellular Inhibition (ADCI) Assay with Affinity Purified Antibodies

To examine whether antibodies specific to OR and SR sequences can exert any parasite growth inhibitory effect, we conducted *in vitro* parasite growth inhibition assays with either murine IgG induced by SE36 or affinity purified human natural IgG specific to OR or SR regions in both direct and human monocyte dependent ADCI assays (Fig. 4). The purified human antibodies were tested for their selectivity and reactivity by ELISA (Fig. S1C, D). No significant direct inhibitory effect was observed in all tested IgG. In contrast, anti-parasitic ADCI activity was strong using either induced murine anti-SE36 IgG or human IgG affinity purified against the two synthetic peptides (OR or SR peptide) (Fig. 4). It is noteworthy that these specific IgG preparation used at final concentration of 0.3 mg/ml have a similar growth inhibitory activity to a 2 mg/ml pool of polyclonal immune African IgG previously used in passive transfer experiments of IgG to malaria patients [27,36]. These results indicate that OR and SR regions are protective epitopes.

Structure Prediction and Physicochemical Characterization of the N-Terminal Domain of SERA5

The structural features of both OR and SR sequences as well as the other parts of SE36 protein (based on the SERA5 N-terminal domain of the Honduras-1 strain) were examined using several structure prediction servers. Consensus Disorder Prediction [34] discriminated ordered and disordered regions in the sequence (Fig. 5 and Fig. S3). The region from the N-terminal end to Asp-76 (Fig. 5) was predicted to be predominantly disordered. This region corresponds to OR and SR sequences which were revealed as protective epitopes inducing antibodies capable of parasite growth inhibition. Other disordered regions identified were the polyserine sequence and its N- and C-terminal adjacent regions (matching series I peptides 7–9). All other parts in SE36 were predicted to be ordered. Using the secondary structure prediction program in NPS@ server [33], the assigned secondary structures matched the ordered regions identified with Consensus Disorder Prediction (Fig. 5). The predictions of ordered regions were further confirmed by the fact that all cysteine residues could be aligned at the same positions and high sequence identity and similarity could be obtained in the relatively conserved region shown in Fig. 5 in all of *Pf*SERA family, suggesting a common tertiary structure among the SERA family proteins (Table 1 and Fig. S3).

The synthetic peptides corresponding to OR and SR regions were subjected to CD experiments to define their structural characteristics. The peptide for the OR region did not show any ability to form rigid, typical secondary structure even in the presence of 40% TFE, an inducer and stabilizer for secondary structure (Fig. 6A–C). The behavior of the SR peptide was similar to OR peptide in the absence of TFE. However, with 40% TFE and at lower temperature, the SR peptide showed spectral change distinct from the OR peptide (Fig. 6D–F). Considering the low complexity due to biased amino acid composition of the SR region and the non-significant spectral change, an intrinsically unstructured nature of the region can be suggested. However, the structure predictions also assigned short ordered structure on a cluster of valines (VSTVSVSQ) in the SR region. These results may suggest a possible role of this region for hydrophobic interaction with other molecule(s).

The CD spectrum of the whole SE36 protein suggests an ordered structure (Fig. 7A). The shoulders near 208 and 222 nm suggest the existence of an α-helical structure. In the above

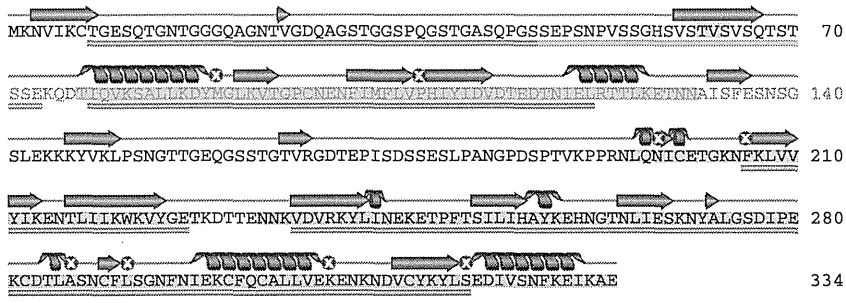

Figure 5. Schematic summary of the sequence analyses of SE36 by structure prediction servers. The shaded amino acids were predicted as ordered residues by the program, Consensus Disorder Prediction. The regions predicted as α-helix and β-structure by NPS@ are represented as helices and arrows above the sequence, respectively. Amino acid denoted by a symbol "⊗"did not reach consensus. The bars in orange, green and brown below the sequence denote OR region, SR region and relatively conserved regions among SERA family genes 1–7 and 9, respectively.
doi:10.1371/journal.pone.0098460.g005